RTN Model for Supply Logistics of Carbon Dioxide in the Field Management for Carbon Capture and Storage

Joelle Guisso[1], Soumya Shikha[1], Alejandro Rodríguez-Martínez[2], Anna Robert[2], Ignacio E. Grossmann[1,*]

[1]Department of Chemical Engineering, Carnegie Mellon University, Pittsburgh, PA 15213
[2]TotalEnergies R&D, 2 place Jean Miller, 92078 Paris La Defense Cedex, France

1. Abstract

We present a mixed-integer linear programming (MILP) model for a maritime inventory routing (MIR) problem for Carbon Capture, Utilization and Storage (CCUS). The model is formulated using an extension of the resource-task network (RTN) representation that minimizes sailing costs. The proposed model can accommodate any number of vessels and emitters. The discrete-time model considers accurate task durations relative to the load of CO_2. The model can generate an hourly inventory profile and detailed scheduling with accurate results. We show the computational performance of the model on five small-scale examples, and on one large-scale real life instance.

2. Introduction

The increase in carbon emissions and the expected further increase in energy consumption is an environmental concern that requires serious solutions. Carbon Capture, Utilization and Storage (CCUS) is a major step for decarbonization of industries and reaching net-zero (IEA[4]). CCUS systems are crucial for retrofitting existing energy plants with CCUS technology. In addition, some industrial sectors are hard to decarbonize without CCUS, including cement and chemicals industries (IEA[4]). Blue hydrogen production, which comprises of 40% of low-carbon hydrogen production, depends on CCUS for decarbonization (IEA[4]). CCUS is also needed for the removal of carbon dioxide from the atmosphere through Direct Air Capture (DAC) (IEA[4]). If net-zero emissions are to be achieved by 2070, about 15% of the cumulative reduction in emissions are covered by CCUS systems, as per the Sustainable Development Scenario. CCUS industrial centers, like Norway's Northern Lights project, merges several CCUS infrastructures to reduce the price and increase efficiency of the deployment of CCUS systems (IEA[4]).

Rigorous supply chain optimization through mixed-integer linear programming (MILP) reduces the cost of transportation and handling of carbon dioxide in CCUS hubs. Transportation

of CO_2 for CCUS systems range from pipelines, shipment, and overland transportation. Depending on the conditions, the optimal transportation system can be chosen. It depends on the distances, the location, and the production rate of CO_2. For long distances, ship-based transportation is favored over pipeline transportation (Decarre et al.[6]). In this model, only ship-based transport is considered for cryogenic CO_2. This paper presents an innovative model to optimize the supply chain of cryogenic CO_2 that is produced from concentrated sources. The model uses the Resource-Task-Network (RTN) MILP formulation (Pantelides[17]) that minimizes the operating expenditure and determines the optimal scheduling of ship-based transport of cryogenic CO_2. The sequestration of cryogenic CO_2 is not addressed in this paper. It can be found in the recent paper by Abhijnan et al.[1] A logistics model is employed to find the most cost-effective usage of the available vessels and of the storage tanks at the terminal port.

This paper is organized as follows. After a review of the literature related to the considered topic, we present the problem statement of the vessel scheduling system, describing the objective function and the assumptions involved. Next, we formulate a mixed-integer linear programming model based on the RTN representation to optimize the shipment transport of CO_2 from the emitters to the terminal port. We exhibit some numerical experiments in the last part of the article along with comments and analysis, before ending with a conclusion and discussion for future works.

3. Literature Review

Maritime shipping has been the mainstay for long distance transportation or for overseas transportation. For decades, models have been developed to optimize the ship routing and scheduling to minimize the cost of shipping. A thorough review of ship routing and scheduling optimization is given by Christiansen et al.[5] CO_2 shipping falls into the category of industrial and tramp shipping. Many aspects within industrial and tramp shipping include ship routing, ship scheduling, fleet optimization, berths scheduling, and emissions minimization from fuel consumption.

Fleet optimization involves determining the optimal number of vessels and the optimal vessel size to minimize the shipping costs. Zeng and Yang[23] developed and solved an integer programming (IP) model integrating fleet optimization for coal shipping using a tabu search algorithm. The

model is able to reduce shipping costs by 21.01% when optimizing the vessel capacity. The difference between shipment routing and scheduling is that the latter has a temporal aspect, involving the specific times of tasks. Brønmo et al.[2] present a heuristic approach to solving a cargo routing and scheduling problem. Li and Pang[14] present a heuristic solution for berth scheduling, allowing only one vessel to load or unload at a port at a time, since the port only has one berth available. Models that also consider inventory management at the ports in addition to vessel routing and scheduling are denoted as maritime inventory routing (MIR) problems.

Song and Furman[20] address a maritime inventory routing (MIR) problem that optimizes the vessels' routing and scheduling given several suppliers and terminals. The model considers berth availability, and hence only one vessel is allowed for each berth at a certain timestep. The model also considers a fixed loading/unloading time duration independent of how much has loaded. Gatica and Miranda[8] develop a ship routing and scheduling optimization with variable sailing speed. Kim et al.[12] present a mixed-integer nonlinear programming (MINLP) model that determines the optimal vessel sailing speed, the amount of bunkering fuel to be purchased, and the optimal number of bunkering ports, minimizing the overall costs, including environmental emissions costs.

A thorough review of optimization methods for short-term scheduling of batch processes is presented by Méndez, Cerda, Grossmann, Harjunkoski, and Fahl[15]. Network-based formulations include the state task network model, developed by Kondili, Pantelides, and Sargent[13] and the resource task network, developed by Pantelides[17]. The STN representation is the foundation for the RTN representation, in which the state, equipment, storage capacity, utilities, and transportation devices are all treated as resources, while in the STN representation, they are treated separately. Hence, the RTN formulation is easier to formulate and relies on three sets of constraints and three types of variables: resource level continuous variables, task occurrence binary variables, and task extent continuous variables (Wassick and Ferrio[21]). Pantelides showed that the integrality gap of RTN formulations is always smaller than the smallest possible integrality gap of an STN formulation (Georgiadis et al.[9]). Both formulations could be based on discrete or continuous time representation (Castro et al. [3]). Floudas and Lin[7] provide an overview of process scheduling models with discrete-time or with continuous-time approaches. Discrete-time formulations yield tighter LP relaxations, while also producing models with a large number of variables specific for each

discrete timestep that increase the problem size and render the problem intractable for a long horizon (Yee and Shah[22]). Discrete-time formulations are only accurate when the timestep is taken to be the greatest common factor of all task durations (Harjunkoski et al.[11]). When a task duration is rounded up to the timestep duration, accuracy decreases. Nie et al.[16] presents an RTN reformulation that "lifts" variables to account for the task occurrence and task extent history.

4. Problem Statement

This paper presents a new formulation for a maritime inventory routing (MIR) problem for CCUS. Given are several emitters (CO_2 capture sites) and a heterogeneous fleet of vessels (CO_2 carriers) (see Figure 1). Each vessel has a sailing speed, cargo loading speed, storage capacity, and fuel consumption. Each emitter has a port location with its cryogenic CO_2 production rate, which can vary at each timestep. Also, the target export rate towards the fields for permanent storage is known. The storage capacity and number of available berths are also known for each emitter port and the terminal port. The model also considers what type of vessels are accepted for each berth, and how many berths are available at each port. The vessel can wait outside the terminal port before sailing to an emitter port. The amount loaded to the vessel determines the loading and unloading times.

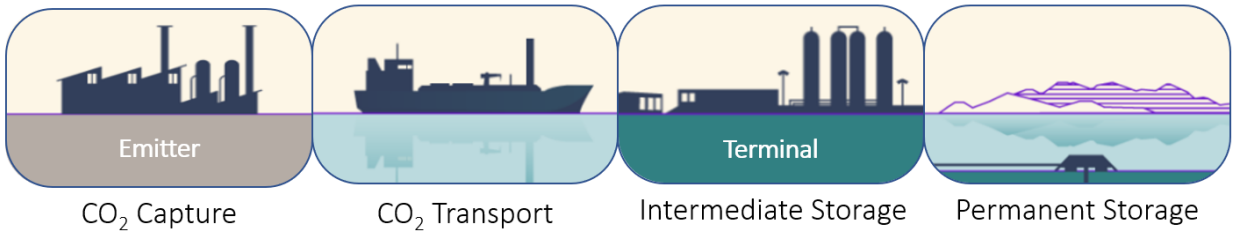

Figure 1: Schematic at the maritime inventory routing for CCUS

The goal is to optimize the shipment scheduling of cryogenic CO_2 from emitters to the onshore terminal. The goal is to maximize the profit, minimizing the operating expenditure and the venting at the emitter ports so as to provide a smooth shipping rate at the terminal port. The profit can be defined as the income from the shipped cryogenic CO_2 minus the fuel costs. The more CO_2 is shipped, the more CO_2 is injected for permanent storage.

The solution of the optimization model indicates which emitter ports the vessel has to visit in each voyage and the amount to be loaded in each voyage from each emitter port. The model should also

determine which vessels are active and which are idling during the entire planning horizon. The operating expenditure includes the fuel consumption of the vessels. The fuel consumption for each vessel is handled by the model. Specifically, it considers that the vessel consumes fuel at a rate depending on the undergoing task and on the type of vessel. Each type of vessel has task-specific costs, e.g., sailing costs, waiting costs, bunkering costs, loading costs, etc. The vessel is allowed to bunker at the injection terminal when needed. The initial location of the vessel is specified at the beginning, either at the injection terminal or at one of the emitters. To develop the optimization model, the following assumptions stated below are made.

It is assumed that 99.99% pure cryogenic carbon dioxide is produced by the emitters. Hence, the model does not consider pre-processing processes such as gas conditioning and liquefaction. It is also assumed that no leakage occurs during shipment. Hence, what is unloaded at the terminal is exactly equal to what has loaded at the emitter. In addition, no boil-off is considered at the injection terminal cryogenic tanks.

At each emitter there is a storage limit for the cryogenic CO_2. If the production exceeds the limit, cryogenic CO_2 must be vented. Hence, the model should optimize the shipment so as to decrease the waiting time at the ports, while also making sure to ship enough cryogenic carbon dioxide to prevent venting at the emitter ports. We assume in the model that there is sufficient amount of CO_2 at the terminal, so it is never depleted.

This model is based on time discretization into a number of time steps of equal duration. One parameter that needs to be determined is the timescale of the model. The accuracy and results of the model greatly depend on the discretization of the time domain. There is a tradeoff between data accuracy and problem tractability. As the duration of the timestep decreases, the accuracy increases. However, the smaller the timestep, the larger the model becomes, and the more detailed the supply schedule to the terminal port. As the time horizon increases, the number of variables increases and hence the computational time increases.

5. Model Formulation

We present in this section an MILP formulation for the shipment scheduling and inventory management of cryogenic CO_2 using an extension of the RTN representation (Pantelides[17]). To clarify, we present a model that could apply to examples with any number of vessels and emitters,

including the example of one vessel and one emitter in Figure 2. In this RTN model, the loading and unloading time depend on the amount that is being loaded. Since the duration of tasks in the RTN representation are fixed, it would not be accurate to fix the duration of the loading and unloading tasks. To be able to produce accurate results, the loading and unloading tasks' durations are fixed to a relatively small duration, which would be the time step of the model, so that the model performs repetitions of the tasks until the desired cryogenic CO_2 is loaded or unloaded. As a result, the amount loaded/unloaded is a multiple of the amount loaded/unloaded in a duration of the timestep. The timestep that yields highest accuracy is the greatest common divisor of the durations of all tasks. In the case studied here, the greatest common divisor assumed is 1 hour. As the timestep increases, the model can solve for longer time horizons in shorter computation times, but at the cost of reduced accuracy. Therefore, we conducted our tests using a timestep of only 1 hour to maintain accuracy.

In an RTN representation, the resources are represented by circular nodes, while the tasks are represented by rectangular nodes. In this model, the resource nodes are used to represent vessels, cryogenic CO_2, or berths, while the task nodes represent sailing to emitter, shipping to terminal, waiting at the terminal, loading, or unloading. The RTN representation for the shipment of cryogenic CO_2 from one emitter to the terminal using one vessel is shown in Figure 2. This RTN representation can be expanded to include more than one vessel and one emitter. The general MILP model equations are presented next.

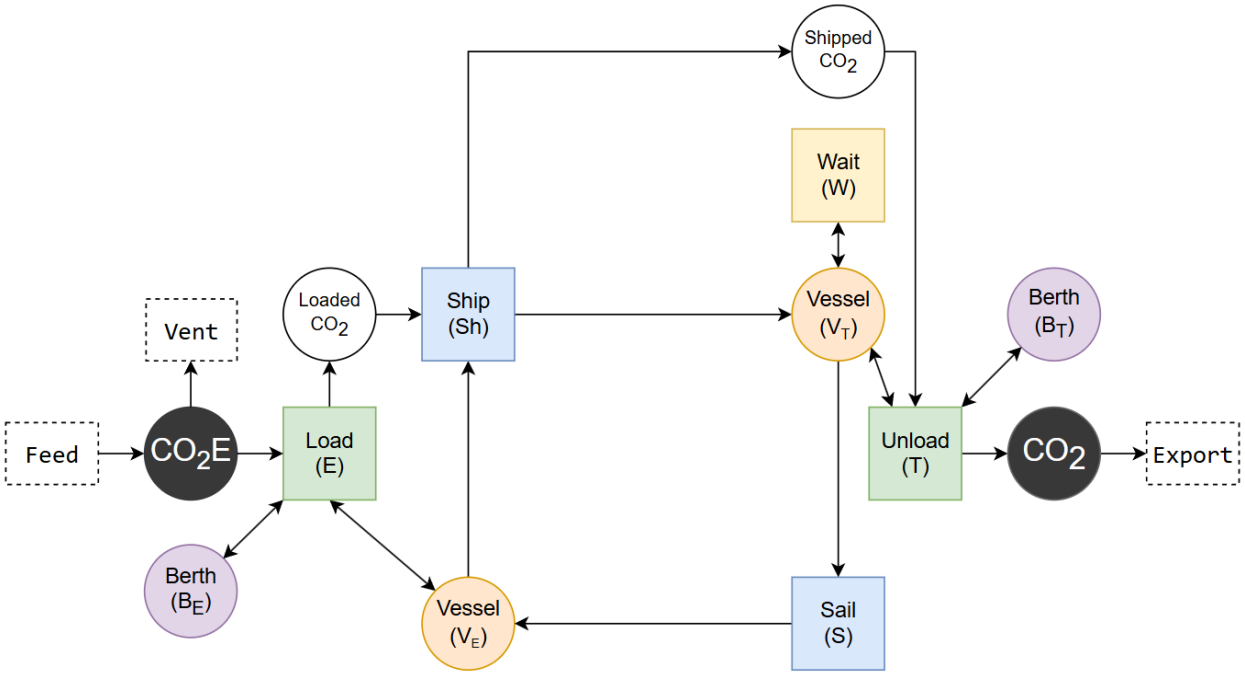

Figure 2: RTN Schematic for 1 Vessel and 1 Emitter Model

The task variables, $N_{task}|_{i,j,t}$, represented by rectangular nodes, are binary, while the resource variables, $R_r|_{i,t}$, represented by circular nodes, are continuous. Resources for vessels could either be at the terminal *(V_T)* or at the emitter *(V_E)*. Resources representing cryogenic CO_2 either refer to the liquid stored in tanks at the emitter port *(CO_2E)*, at the terminal *(CO_2)*, or in the vessel before shipping *(Loaded CO_2)* and after shipping *(Shipped CO_2)*. The node denoted by *Feed* represents a fixed parameter that represents the production rate of the emitter. The node denoted by *Export*, representing the target export rate, is a fixed parameter only when the level in the tank is above 25% capacity. The node denoted by *Vent* is a variable which represents the cryogenic CO_2 vented at timestep t, which should be minimized and ideally set to zero.

The vessel sails from the terminal port to the emitter using the task *Sail (S)*. The vessel loads CO_2 using the task *Load (E)*. Then, the vessel ships to the terminal port using task *Ship (Sh)* and unloads using task *Unload (T)*. The vessel can wait at the terminal using the task *Wait (W)*. This task can only be activated if the vessel has completely unloaded all of the CO_2, so as to not allow intermittent loading/unloading. For any given set of vessels and emitters, the model can be represented with a general set of constraints, which are the resource balances, resource limits, and operational constraints.

1. Resource Balances

The cryogenic CO_2 level at emitter port i and at time step t is represented by the resource $R_{CO_2E,i,t}$. At each time step, the level is updated by adding the production rate, $\Pi^{in}_{CO_2E,i,t}$, and by subtracting the loaded cryogenic CO_2 into vessel j at time step $t-1$, $\xi_{E,i,j,t-1}$. If the level reaches its upper limit, an amount of cryogenic CO_2 would be vented at timestep t, represented by $\Pi^{out}_{CO_2E,i,t}$.

$$R_{CO_2E,i,t} = R^{init}_{CO_2E,i,t}\big|_{t=1} + R_{CO_2E,i,t-1}\big|_{t>1} - \sum_{j\in J} \xi_{E,i,j,t-1}\big|_{t>1} + \Pi^{in}_{CO_2E,i,t} - \Pi^{out}_{CO_2E,i,t} \qquad \forall i \in I,\ \forall t \in TS \tag{1}$$

The resource of the berth at the emitter port i, represented by $R_{B_E}\big|_{i,t}$, is consumed at time step t if any vessel begins loading cryogenic CO_2 at the same time, as shown in Equation (2). The resource of the berth is produced when the task for loading *(E)* ends. As mentioned previously, the duration of the task for loading or unloading is one timestep. If the emitter port has a single berth available for loading, then the resource limit would be 1, and only 1 vessel is allowed to load at a specific time step t. Before and after loading, a specific time is allocated for mooring and installing the ramp for loading, during which the berth is occupied by the vessel. In this model, 2 hours are considered for mooring, and 1 hour is considered for ramp installation. The model should also consider the time for unmooring and ramp removal. Hence, the berth would be occupied for an additional 6 hours before and after loading cryogenic CO_2. Nevertheless, in the model it was found to be much easier and simpler to consider these operations to take place right before shipping to the terminal port. The possible values that $R_{B_E,i,t}$ can take are discrete values since berths are consumed and produced in discrete quantities by the task for loading *(E)*. Hence, there is no need to define the resource variable as discrete (Perez et al.[18]).

$$R_{B_E,i,t} = R^{init}_{B_E,i,t}\big|_{t=1} + R_{B_E,i,t-1}\big|_{t>1} + \sum_{j\in J}\left(N_{E,i,j,t-1}\big|_{t>1} - N_{E,i,j,t}\right) + \sum_{j\in J}\left(N_{Sh,i,j,t-\tau_{BO}}\big|_{t>\tau_{BO}} - N_{Sh,i,j,t}\right) \qquad \forall i \in I,\ \forall t \in TS \tag{2}$$

Vessel j at the emitter i at timestep t, represented by the resource $R_{V_E,i,j,t}$, which is equated to zero, is given in Equation (3). Since resource variables are nonnegative, this resource is set to zero

always, and hence it is not a variable. $R^{init}_{V_E,i,j,t}\big|_{t=1}$ represents the initial condition of vessel j at emitter i. If the initial location of vessel j is at emitter i, then the parameter is 1. The equation is governed by four tasks: sailing from terminal port to emitter i, idling at emitter i, loading, shipping to terminal port. The task durations for idling at emitter and for loading are set to one timestep, while the task durations for sailing to emitter i and shipping to terminal port, denoted by $\tau_{s,i}$, depend on the distance from emitter i to the terminal port and on the vessel nominal speed.

$$R_{V_E,i,j,t} = R^{init}_{V_E,i,j,t}\big|_{t=1} + R_{V_E,i,j,t-1}\big|_{t>1} + N_{S,i,j,t-\tau_{s,i}}\big|_{t>\tau_{s,i}} - N_{E,i,j,t} + N_{E,i,j,t-1}\big|_{t>1} - N_{Sh,i,j,t} - N_{IE,i,j,t} + N_{IE,i,j,t-1}\big|_{t>1} \quad \begin{matrix} \forall i \in I \\ \forall j \in J \\ \forall t \in TS \end{matrix} \quad (3)$$

The amount loaded in the vessel is governed by the extents of two tasks: *Load (E)* and *Ship (Sh)*. *Load (E)* produces cryogenic CO_2 in vessel j after one timestep, which is represented by $R_{L,i,j,t}$ in Equation (4). The cryogenic CO_2 is consumed by task *Ship (Sh)* at the start of timestep t. The extents are continuous variables that represent how much cryogenic CO_2 is loaded or shipped: $\xi_{Sh,i,j,t}$ is the cryogenic CO_2 that has been shipped to the terminal port at time step t.

$$R_{L,i,j,t} = R^{init}_{L,i,j,t}\big|_{t=1} + R_{L,i,j,t-1}\big|_{t>1} + \xi_{E,i,j,t-1}\big|_{t>1} - \xi_{Sh,i,j,t} \quad \begin{matrix} \forall i \in I \\ \forall j \in J \\ \forall t \in TS \end{matrix} \quad (4)$$

The resource that represents vessel j at the terminal port at timestep t is given by $R_{V_T,j,t}$, which has an upper bound of zero, which means that this resource is always set to zero, similar to $R_{V_E,i,j,t}$. At $t = 1$, if vessel j is at the injection terminal, then $R^{init}_{V_T,j,t}\big|_{t=1} = 1$. This forces the vessel to be consumed by a task in the next timestep, which is either *Wait (W)*, *Unload (T)*, or *Sail (S)*. The tasks *Wait (W)* and *Unload (T)* both have a time duration of 1 timestep. The task *Ship (Sh)* consumes vessel j at emitter i and produces it at the terminal port after the shipment duration, $\tau_{s,i}$.

$$R_{V_T,j,t} = R^{init}_{V_T,j,t}\big|_{t=1} + R_{V_T,j,t-1}\big|_{t>1} + \sum_{i\in I} N_{Sh,i,j,t-\tau_{s,i}}\big|_{t>\tau_{s,i}} - N_{T,j,t} + N_{T,j,t-1}\big|_{t>1} - N_{W,j,t} + N_{W,j,t-1}\big|_{t>1} - \sum_{i\in I} N_{S,i,j,t} - N_{IT,j,t} + N_{IT,j,t-1}\big|_{t>1} \quad \begin{matrix} \forall j \in J \\ \forall t \in TS \end{matrix} \quad (5)$$

Task *Ship (Sh)* also produces shipped cryogenic CO_2, which is represented by the resource $R_{Shipped}\big|_{j,t}$. The shipped cryogenic CO_2 is consumed when vessel j unloads the cryogenic CO_2 at the terminal port directly upon arrival of the vessel to the port. This is represented by the extent of task *Unload (T)*: $\xi_{T,j,t}$. The extent depends on how much is unloaded during the timestep. It is discretized based on the loading speed and timescale of the model.

$$R_{Shipped,j,t} = R^{init}_{Shipped,j,t}\big|_{t=1} + R_{Shipped,j,t-1}\big|_{t>1} + \sum_{i\in I}\xi_{Sh,i,j,t-\tau_{s,i}}\big|_{t>\tau_{s,i}} - \xi_{T,j,t} \qquad \forall j \in J,\ \forall t \in TS \quad (6)$$

Similar to the berth resource at the emitter, the upper bound for the berth resource at the terminal port depends on how many berths are available at the terminal. One berth is consumed when vessel j unloads at the terminal port at the beginning of timestep t. The berth becomes available at the end of the timestep. If vessel j has not unloaded completely, the task *Unload (T)* repeats and consumes the berth again. The berth is also consumed during mooring, connection, unmooring and disconnection, which take a total of approximately 6 hours before and after unloading. We account for this time, represented by τ_{BO}, before the vessel reaches the terminal, i.e., 6 hours before the shipping task ends.

$$R_{B_T,t} = R^{init}_{B_T,t}\big|_{t=1} + R_{B_T,t-1}\big|_{t>1} - \sum_{j\in J} N_{T,j,t} + \sum_{j\in J} N_{T,j,t-1}\big|_{t>1} + \sum_{i\in I}\sum_{j\in J}\left(N_{Sh,i,j,t-\tau_{s,i}}\big|_{t>\tau_{s,i}} - N_{Sh,i,j,t-(\tau_{s,i}-\tau_{BO})}\big|_{t>\tau_{s,i}-\tau_{BO}}\right) \qquad \forall t \in TS \quad (7)$$

The cryogenic CO_2 level at the terminal port tanks at the beginning of timestep t is given by the resource $R_{CO_2,t}$, which has an upper bound of the terminal port storage capacity C_T. The level increases if vessel j unloads at time step $t-1$. $\Pi^{out}_{CO_2,t}$ is the injection flow of cryogenic CO_2 from the storage tanks to the buffer tank that governs the flow into the wells.

$$R_{CO_2,t} = R^{init}_{CO_2,t}\big|_{t=1} + R_{CO_2,t-1}\big|_{t>1} + \sum_{j\in J}\xi_{T,j,t-1}\big|_{t>1} - \Pi^{out}_{CO_2,t-1} \quad \forall t \in TS \quad (8)$$

2. Resource Limit Constraints:

Resource limit constraints provide an upper bound for the resource variables. They are given by Equations (9)-(16). The resource of cryogenic CO_2 at the emitter port is bounded by the storage capacity at the emitter, C_i. Equations (11) and (13) certify that the vessel resources at the terminal or emitter port are always zero. This is because the resource must be directly consumed after being produced by a task, to prevent unallowed waiting during loading or unloading. The resources of the loaded amount and shipped amount are bounded by the vessel capacity C_j.

$$\left.\begin{aligned} R_{CO_2E,i,t} &\le C_i \\ R_{B_E,i,t} &\le B_E^{max} \end{aligned}\right\} \ \forall i \in I, t \in TS \tag{9}$$

(10)

$$\left.\begin{aligned} R_{V_E,i,j,t} &= 0 \\ R_{L,i,j,t} &\le C_j \end{aligned}\right\} \ \forall i \in I, j \in J, t \in TS \tag{11}$$

(12)

$$\left.\begin{aligned} R_{V_T,j,t} &= 0 \\ R_{Shipped,j,t} &\le C_j \end{aligned}\right\} \ \forall j \in J, t \in TS \tag{13}$$

(14)

$$\left.\begin{aligned} R_{B_T,t} &\le B_T^{max} \\ R_{CO_2,t} &\le C_T \end{aligned}\right\} \ \forall t \in TS \tag{15}$$

(16)

3. Operational constraints:

The last set of constraints for the RTN are operational constraints for loading, shipping, and unloading, which are given by Equations (17)-(19), respectively. TI represents the time interval duration and PS_j represents the loading speed of vessel j. The extent of the task is nonzero only if the occurrence of the respective task is one. An extent of a task represents how much is involved in a task if it is active. For example, if $N_{E,i,j,t}$ is zero, then $\xi_{E,i,j,t}$ is zero too.

$$\left.\begin{aligned} \xi_{E,i,j,t} &\le TI \times LS_j \times N_{E,i,j,t} \\ \xi_{Sh,i,j,t} &\le C_j \times N_{Sh,i,j,t} \end{aligned}\right\} \ \forall i \in I, j \in J, t \in TS \tag{17}$$

(18)

$$\xi_{T,j,t} \le TI \times LS_j \times N_{T,j,t} \ \ \forall j \in J, t \in TS \tag{19}$$

4. Additional Constraints:

To account for the fuel expenses of the transportation, more variables are added into the model. A resource variable is assigned for the fuel level in the bunker tanks of vessel j at timestep t. A task variable is introduced to account for bunkering of vessel j at timestep t. Finally, a resource variable

is introduced for the available fuel at the terminal to feed the bunkering of the vessel. The bunkered fuel is consumed by all the tasks of the model, except for idling (IE or IT). The updated RTN model is shown in Figure 3. The tasks for Idling at Terminal (IT) or Idling at Emitter (IE) are not shown in the figure since this network is for one vessel only, hence the vessel cannot idle.

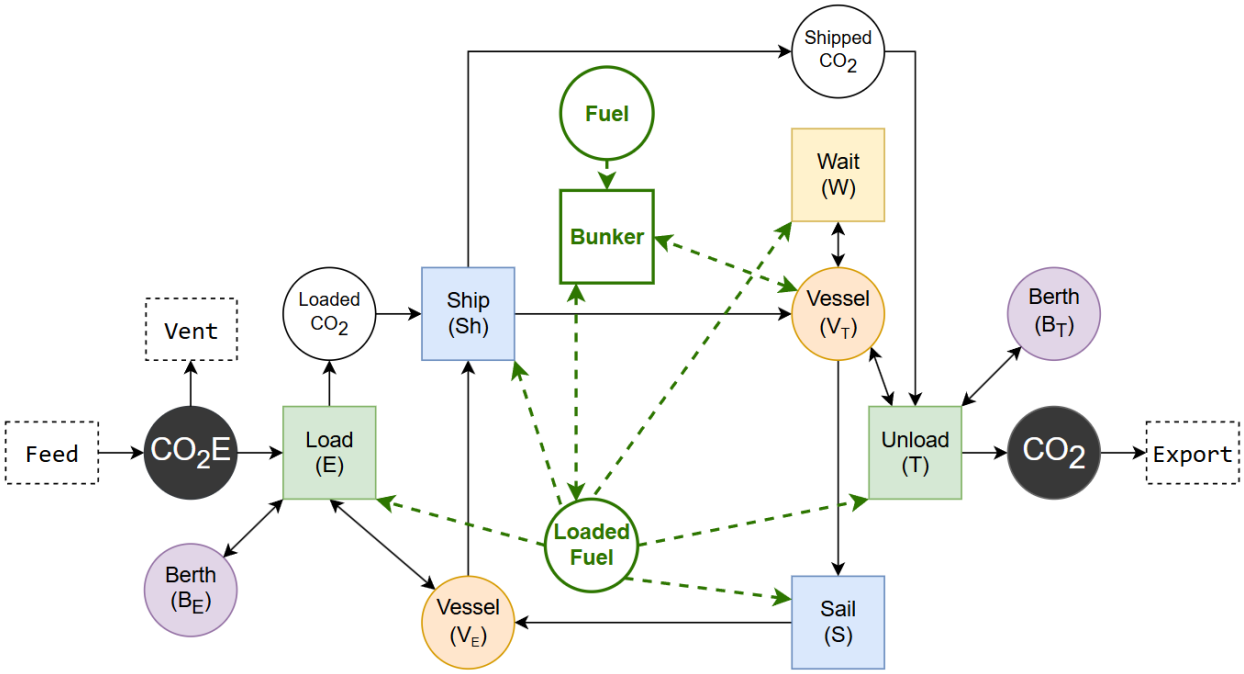

Figure 3: Detailed RTN Schematic for 1 Vessel and 1 Emitter Model

Equation (20) represents the loaded fuel resource in vessel j at each timestep t. The loaded fuel resource in vessel j is bounded by the bunker tank capacity of vessel j, as shown in Equation (21). The fuel consumption of vessel j at timestep t, $FC_{j,t}$, which is given by Equation (22), depends on which task is active. When the task *Ship (Sh)* is active at timestep t', the timesteps during which the vessel is sailing is during ST_i when the vessel sails from the Pilot Boarding Point of emitter i (PBP_i) to that of the injection terminal port (PBP_T), as shown in the timeline in Figure 4. Hence, Equation (22) considers only timesteps within ST_i to calculate the fuel consumption during sailing. The timesteps accounted for when the vessel starts sailing and reaches PBP_i represent waiting for the pilot and tug out, channeling time (CT_i), unmooring and disconnection, ramping out, and contingency. Channeling time (CT_i) is specific for each emitter port.

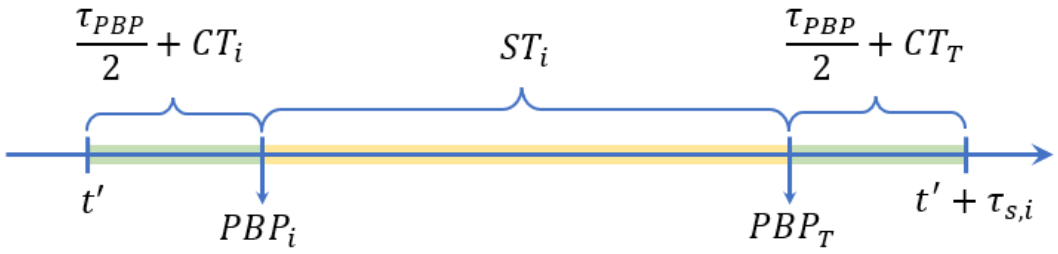

Figure 4: Timeline when the vessel starts sailing from Emitter i at timestep t'

Equation (23) is the resource balance constraint for the available fuel level at the terminal. Equation (24) fixes the extent variable of bunkering to zero if the bunkering task is not triggered (i.e., $N_B|_{j,t} = 0$). Equation (25) represents the fuel costs to be minimized. FP is the current fuel price of 1 ton of LNG in USD.

$$\left.\begin{aligned} R_{LF,j,t} = R^{init}_{LF,j,t}\big|_{t=1} + R_{LF,j,t-1}\big|_{t>1} + \sum_{j\in J}\xi_{B,j,t-1}\big|_{t>1} - FC_{j,t} \\ R_{LF,j,t} \le BT_j \end{aligned}\right\} \quad \forall j \in J, t \in TS \tag{20}$$

(21)

$$\begin{aligned} FC_{j,t} = [C_{S,j}] * \sum_{i\in I}\left[\sum_{t'}\left(N_{S,i,j,t'} + N_{Sh,i,j,t'}\right)\right] \\ + C_{E,j} * \sum_{i} N_{E,i,j,t} + C_{T,j} * N_{T,j,t} + C_{W,j} * N_{W,j,t} \\ + C_{Ch,j} * \left[\sum_{i\in I}(CT_i + CT_T) * \left(N_{S,i,j,t} + N_{Sh,i,j,t}\right)\right] \\ + C_{M,j} * 2\tau_M * \left[\sum_{i\in I}\left(N_{S,i,j,t} + N_{Sh,i,j,t}\right)\right] + C_{B,j} * N_{B,j,t} + C_{Co,j} * z_j \end{aligned} \tag{22}$$

$\forall j \in J$
$\forall t \in TS$
$\forall t' \le t - \frac{\tau_{PBP}}{2} - CT_i$
$\forall t' \ge t - \frac{\tau_{PBP}}{2} - ST_i - CT_i$

$$R_{F,t} = R^{init}_{F,t}\big|_{t=1} + R_{F,t-1}\big|_{t>1} + \Pi^{in}_{fuel} - \sum_{j\in J}\xi_{B,j,t} \quad \forall\, t \in TP \tag{23}$$

$$\xi_{B,j,t} \le BT_j \times N_{B,j,t} \quad \forall j \in J, t \in TS \tag{24}$$

$$OPEX_{j,t} = FP * FC_{j,t} \quad \forall j \in J, t \in TS \tag{25}$$

With this model, nothing prevents the vessel to wait during unloading, or to unload incompletely. To prevent intermittent unloading, a resource variable for the vessel capacity is added to the model. This resource variable would model the available capacity in vessel j at timestep t. This would

only allow waiting, bunkering, or sailing after the vessel unloads completely. The resource balance constraint for the vessel capacity is given by Equation (26).

$$R_{CAP,j,t} = C_j + R_{CAP,j,t-1}\big|_{t>1} + \xi_{T,j,t-1}\big|_{t>1} - \sum_{i\in I} \xi_{E,i,j,t} \qquad \forall j \in J,\ \forall t \in TS \tag{26}$$
$$+C_j\left[-N_{W,j,t} + N_{W,j,t-1}\big|_{t>1} - N_{B,j,t} + N_{B,j,t-1}\big|_{t>1} + \sum_{i\in I}\left(-N_{S,i,j,t} + N_{S,i,j,t-\tau_{s,i}}\big|_{t>\tau_{s,i}}\right)\right]$$

The resource limit constraint for the vessel capacity is given by Equation (27).

$$R_{CAP,j,t} \le C_j \quad \forall j \in J, t \in TS \tag{27}$$

5. Extension to the Model:

Vessel Activity:

The model minimizes the number of vessels used to complete the operation of transporting cryogenic CO_2 for a certain horizon. We have extended the RTN model to include a binary variable that determines whether a vessel has been active or not.. Equation (28) indicates that if any task excluding IE or IT is active at timestep t, then the binary variable $y_{i,j}$ is 1. Equation (29) states that if $y_{i,j}$ is 1, then vessel j is active. Equation (30) strictly disallows vessel j to idle at the emitter or at the terminal port if it is active. As shown in Equation (22), the vessel does not consume fuel if it is idling (IE or IT). Hence, while minimizing fuel costs, the model optimizes the number of vessels active.

$$\sum_{task} N_{task,i,j,t} \le y_{i,j} \quad \forall i \in I, j \in J, t \in TS, task \notin \{IE, IT\} \tag{28}$$

$$y_{i,j} \le z_j \quad \forall i \in I, j \in J \tag{29}$$

$$N_{IT,j,t} + \sum_{i\in I} N_{IE,i,j,t} \le 1 - z_j \quad \forall j \in J, t \in TS \tag{30}$$

Vessel Assignment:

There might be cases in which vessels need to be assigned apriori to the emitters. One of these cases is when an emitter's berth only accepts small or large vessels. Hence, the large vessels are not allowed to visit any emitter that does not accept large vessels as shown in Equation (31).

$$N_{task,i,j,t} = 0 \quad \forall \left\{ i \in I^{sv} \cap j \in J^{lv} \right\} \cup \forall \left\{ i \in I^{lv} \cap j \in J^{sv} \right\} \tag{31}$$

Terminal Storage Tank Level:

To avoid injection shutdown due to low inventory in the tanks, if the terminal storage tank level drops below 25%, the target injection flow rate should also be reduced to 25% of the normal flow rate, which is set to be the sum of production flow rates of all emitters. The formulation is given by the disjunction in Equation (32) where ε is a small positive tolerance.

$$\begin{bmatrix} x_t \\ R_{CO_2,t} \leq 0.25 C_T \\ \Pi^{out}_{CO_2,t} = 0.25 \sum_{i \in I} \Pi^{in}_{CO_2E,i,t} \end{bmatrix} \bigvee \begin{bmatrix} \neg x_t \\ R_{CO_2,t} \geq 0.25 C_T + \varepsilon \\ \Pi^{out}_{CO_2,t} = \sum_{i \in I} \Pi^{in}_{CO_2E,i,t} \end{bmatrix} \quad \forall t \in TS \tag{32}$$

The disjunction can be reformulated using the Big-M reformulation, as shown in Equation (33). The first equation in the formulation ensures $x_t = 1$ if $R_{CO_2,t} \leq 0.25 C_T$. The second equation ensures that if $x_t = 1$ then $R_{CO_2,t} \leq 0.25 C_T$. The last equation sets the injection flow rate to 25% of the normal flow rate if $x_t = 1$.

$$\left.\begin{aligned} 0.25 C_T - R_{CO_2,t} + \varepsilon &\leq 0.25 C_T * x_t \\ R_{CO_2,t} - 0.25 C_T &\leq 0.75 C_T * (1 - x_t) \\ \Pi^{out}_{CO_2,t} &= (1 - 0.75 * x_t) \sum_{i \in I} \Pi^{in}_{CO_2E,i,t} \end{aligned}\right\} \forall t \in TS \tag{33}$$

The disjunction can also be reformulated using the convex hull reformulation (Grossmann and Trespalacios[10]), as shown in Equation (34).

$$\left.\begin{aligned} R_{GCO_2,t} &\geq 0.25 C_T (1 - x_t) \\ R_{GCO_2,t} &\leq C_T * (1 - x_t) \\ R_{LCO_2,t} &\leq 0.25 C_T x_t \\ \Pi^{out}_{GCO_2,t} &= (1 - x_t) \sum_{i \in I} \Pi^{in}_{CO_2E,i,t} \\ \Pi^{out}_{LCO_2,t} &= 0.25 * x_{L,t} \sum_{i \in I} \Pi^{in}_{CO_2E,i,t} \end{aligned}\right\} \forall t \in TS$$

$$\left.\begin{aligned} R_{CO_2,t} &= R_{GCO_2,t} + R_{LCO_2,t} \\ \Pi^{out}_{CO_2,t} &= \Pi^{out}_{GCO_2,t} + \Pi^{out}_{LCO_2,t} \end{aligned}\right\} \forall t \in TS \tag{34}$$

Objective function: The goal of the mathematical program is to maximize the profit of the CCS project over a specific time horizon, by maximizing the transport of cryogenic CO_2 to the terminal and minimizing the operating expenditure related to the shipment of cryogenic CO_2 and the number of vessels used in the operation. The venting at each emitter is also penalized since it is highly unfavorable to get results with any loss of cryogenic CO_2. The objective function is given by Equation (35). β is taken to be a very large number (100,000 €/kt). The value α is taken to be 40,000 €/kt.

$$\max \phi = \left(\alpha \sum_{t=1}^{H-1} \sum_{j \in J} \xi_{X,j,t} - \beta \sum_{i \in I} \sum_{t \in T} \Pi^{out}_{CO_2E,i,t} - \sum_{j \in J} \sum_{t \in T} OPEX_{j,t} \right) / 1000 \tag{35}$$

The discrete-time RTN model for any number of vessels and emitters is given by Equations (1)-(32), (34) and (35). The fully constructed network for one vessel and one emitter is shown in Figure 5.

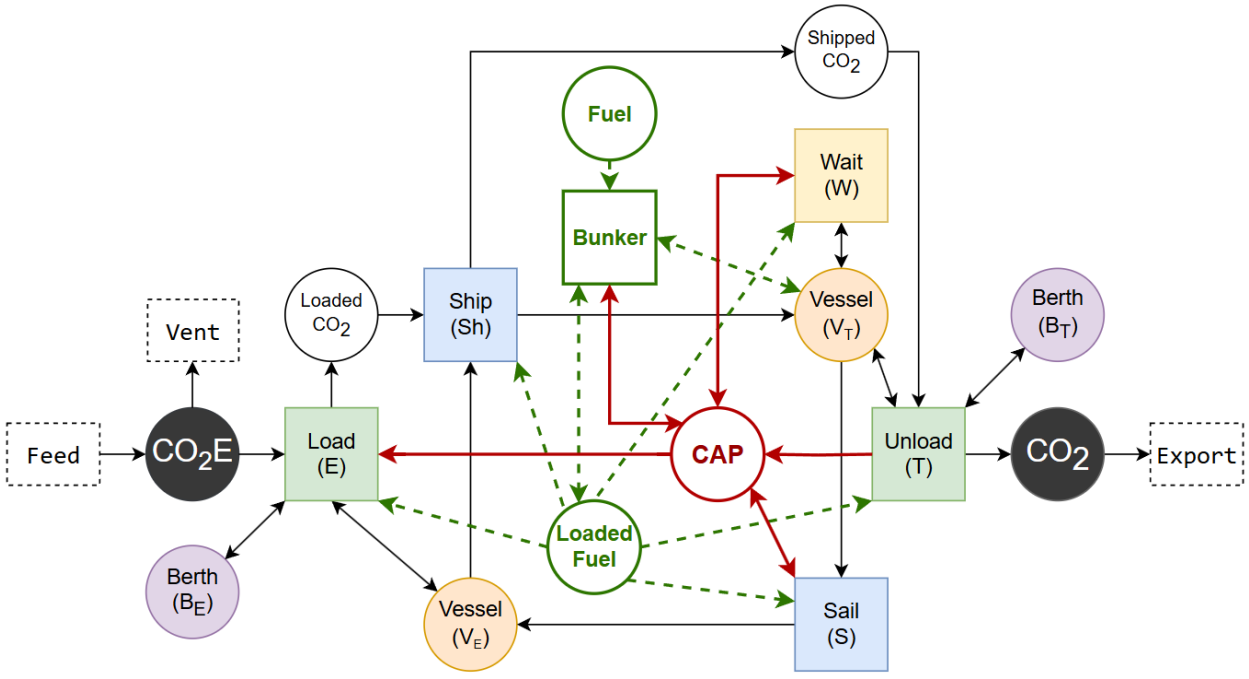

Figure 5: Fully Constructed RTN Schematic for 1 Vessel and 1 Emitter Model

The RTN model could be applied to any number of vessels and emitters but visualizing the network for a larger instance would be hard. Hence, we only present the network for an RTN model with 2

vessels (1&2) and 2 emitters (A&B) as shown in Figure 6. For simplicity, $R_{CAP,j,t}$ and the resources and the task related to bunkering are not shown in Figure 6.

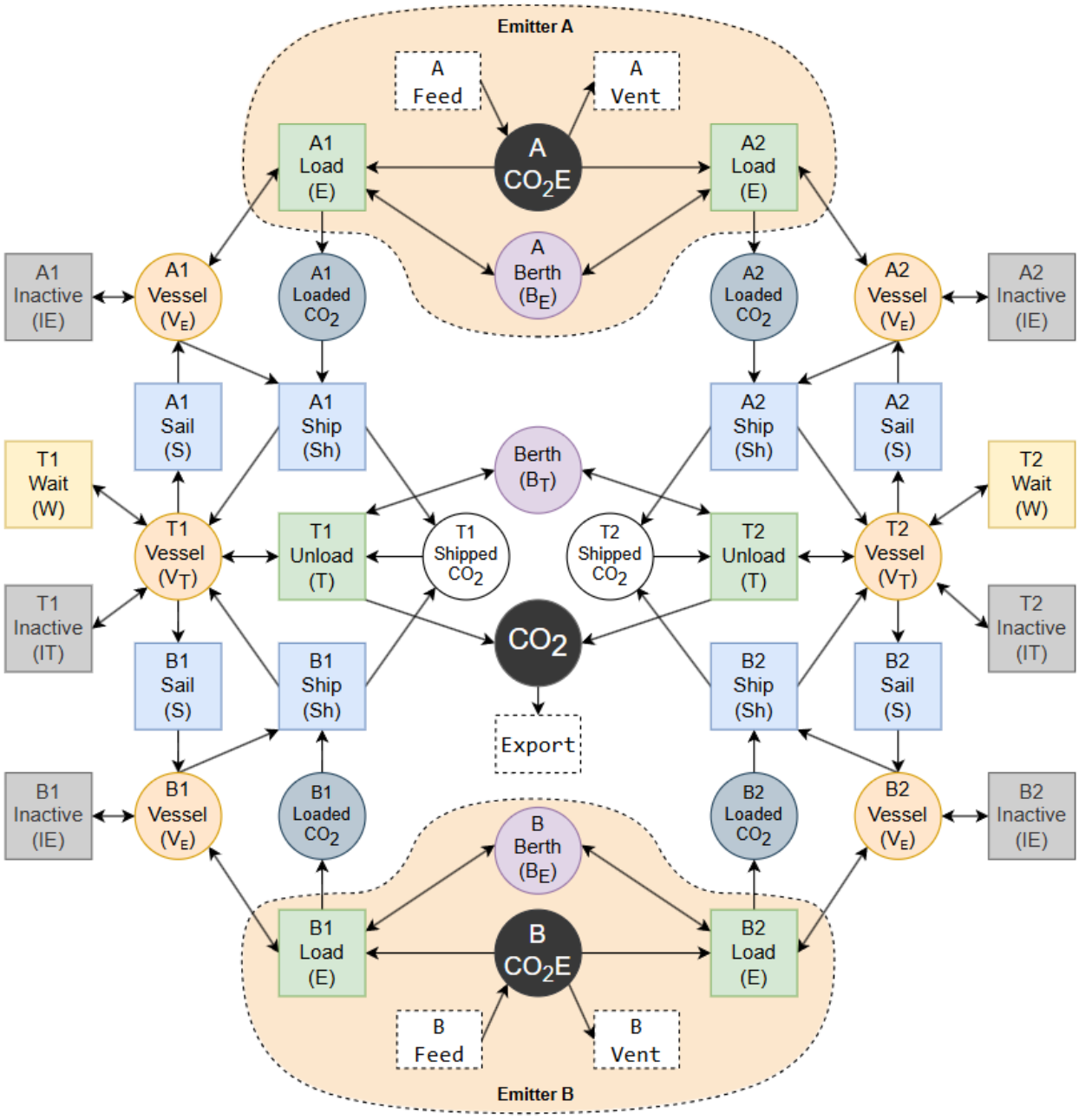

Figure 6: RTN schematic for 2 Vessels and 2 Emitters Model

Model With Milk Runs:

The model with milk runs allows a vessel to load at more than one emitter before shipping to the injection terminal port. The task for "Milk Run" is assigned for each pair of vessel and emitter. If the task is active at timestep t, the task consumes the vessel and the loaded CO_2 at one emitter and produces them at another emitter after the transportation duration. For example, the task "A1 Milk Run" consumes Vessel 1 at Emitter A and the Loaded CO_2 in Vessel 1 and produces them at Emitter B, which become "B1 Vessel" and "B1 Loaded CO_2". After Vessel 1 finishes loading at Emitter B, it leaves to the terminal port through task "B1 Ship", which produces "T1 Vessel" and "T1 Shipped CO_2". These resources, along with "Berth", would be consumed by task "T1 Unload" at the terminal port. This task would produce "CO_2" at the terminal port. Equations (2)-(4) and (23) are replaced by Equations (36)-(40), and (42). Equation (39) is added for the operational constraint for performing milk runs. $N_{MR}|_{i,i',j,t}$ represents the task for sailing from emitter i to emitter i', and $\tau_{i,i'}$ represents the timesteps needed for traveling from emitter i to emitter i'. Figure 7 represents a schematic that allows for milk runs for two vessels (1&2) and two emitters (A&B). Figure 8 depicts the RTN model for that example.

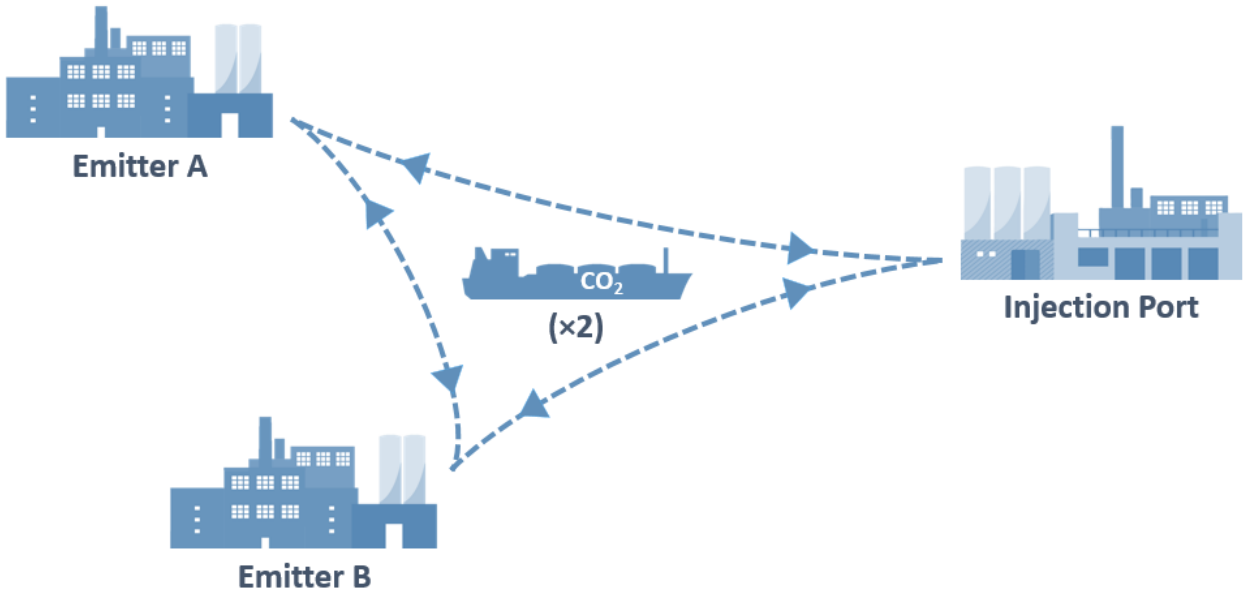

Figure 7: Maritime Shipment Schematic for 2 Vessels and 2 Emitters Model with Milk Runs

$$R_{B_E,i,t} = R^{init}_{B_E,i,t}\big|_{t=1} + R_{B_E,i,t-1}\big|_{t>1} + \sum_{j\in J}\left(N_{E,i,j,t-1}\big|_{t>1} - N_{E,i,j,t}\right) + \sum_{j\in J}\left(N_{Sh,i,j,t-\tau_{BO}}\big|_{t>\tau_{BO}} - N_{Sh,i,j,t}\right) + \sum_{j\in J}\sum_{i'\neq i}\left(N_{MR,i,i',j,t-\tau_{BO}}\big|_{t>\tau_{BO}} - N_{MR,i,i',j,t}\right) \quad \forall i\in I,\ \forall t\in TS \tag{36}$$

$$R_{V_E,i,j,t} = R^{init}_{V_E,i,j,t}\big|_{t=1} + R_{V_E,i,j,t-1}\big|_{t>1} + N_{S,i,j,t-\tau_{s,i}}\big|_{t>\tau_{s,i}} - N_{E,i,j,t} + N_{E,i,j,t-1}\big|_{t>1} - N_{Sh,i,j,t} + \sum_{i'\neq i}\left(N_{MR,i',i,j,t-\tau_{i',i}}\big|_{t>\tau_{i',i}} - N_{MR,i,i',j,t}\right) - N_{IE,i,j,t} + N_{IE,i,j,t-1}\big|_{t>1} \quad \forall i\in I,\ \forall j\in J,\ \forall t\in TS \tag{37}$$

$$R_{L,i,j,t} = R^{init}_{L,i,j,t}\big|_{t=1} + R_{L,i,j,t-1}\big|_{t>1} + \xi_{E,i,j,t-1}\big|_{t>1} - \xi_{Sh,i,j,t} + \sum_{i'\neq i}\left(\xi_{MR,i',i,j,t-\tau_{i',i}}\Big|_{t>\tau_{i',i}} - \xi_{MR,i,i',j,t}\right) \quad \forall i\in I,\ \forall j\in J,\ \forall t\in TS \tag{38}$$

$$\xi_{MR,i,i',j,t} \le C_j \times N_{MR,i,i',j,t}\ \forall i,i'\in I, j\in J, t\in TS, i'\neq i \tag{39}$$

$$FC_{j,t} = C_{S,j} * \sum_{i\in I}\left[\sum_{t'}\left(N_{S,i,j,t'} + N_{Sh,i,j,t'}\right) + \sum_{i'\neq i}\tau_{i,i'}\,N_{MR,i,i',j,t''}\right] + C_{E,j} * \sum_{i\in I} N_{E,i,j,t} + C_{T,j} * N_{T,j,t} + C_{W,j} * N_{W,j,t} + C_{Ch,j} * \sum_{i\in I}\left[(CT_i + CT_T) * \left(N_{S,i,j,t} + N_{Sh,i,j,t}\right) + \sum_{i'\neq i}(CT_i + CT_{i'}) * \left(N_{MR,i,i',j,t}\right)\right] + C_{M,j} * 2\tau_M * \sum_{i\in I}\left[\left(N_{S,i,j,t} + N_{Sh,i,j,t}\right) + \sum_{i'\neq i}\left(N_{MR,i,i',j,t}\right)\right] + C_{B,j} * N_B|_{j,t} + C_{Co,j} * z_j \tag{40}$$

$$\forall j\in J,\ \forall t\in TS$$

$$\forall t' \le t - \frac{\tau_{PBP}}{2} - CT_i$$

$$\forall t' \ge t - \frac{\tau_{PBP}}{2} - ST_i - CT_i$$

$$\forall t'' \le t - \frac{\tau_{PBP}}{2} - CT_i$$

$$\forall t'' \ge t - \frac{\tau_{PBP}}{2} - ST_{i,i'} - CT_i$$

A vessel must not perform milk runs consecutively without loading. This could happen when the inventory level at an emitter is low, so the vessel would sail to another emitter and sail back without

loading CO_2. This could be enforced by a logical implication in Equation (41), which is reformulated into a constraint in Equation (42).

$$N_{MR,i,i',j,t-\tau_{i,i'}} \Rightarrow \neg N_{MR,i',i,j,t} \quad \forall i, i' \in I, i' \neq i, j \in J, t > \tau_{i,i'} \tag{41}$$

$$N_{MR,i,i',j,t-\tau_{i,i'}} + N_{MR,i',i,j,t} \leq 1 \quad \forall i, i' \in I, i' \neq i, j \in J, t > \tau_{i,i'} \tag{42}$$

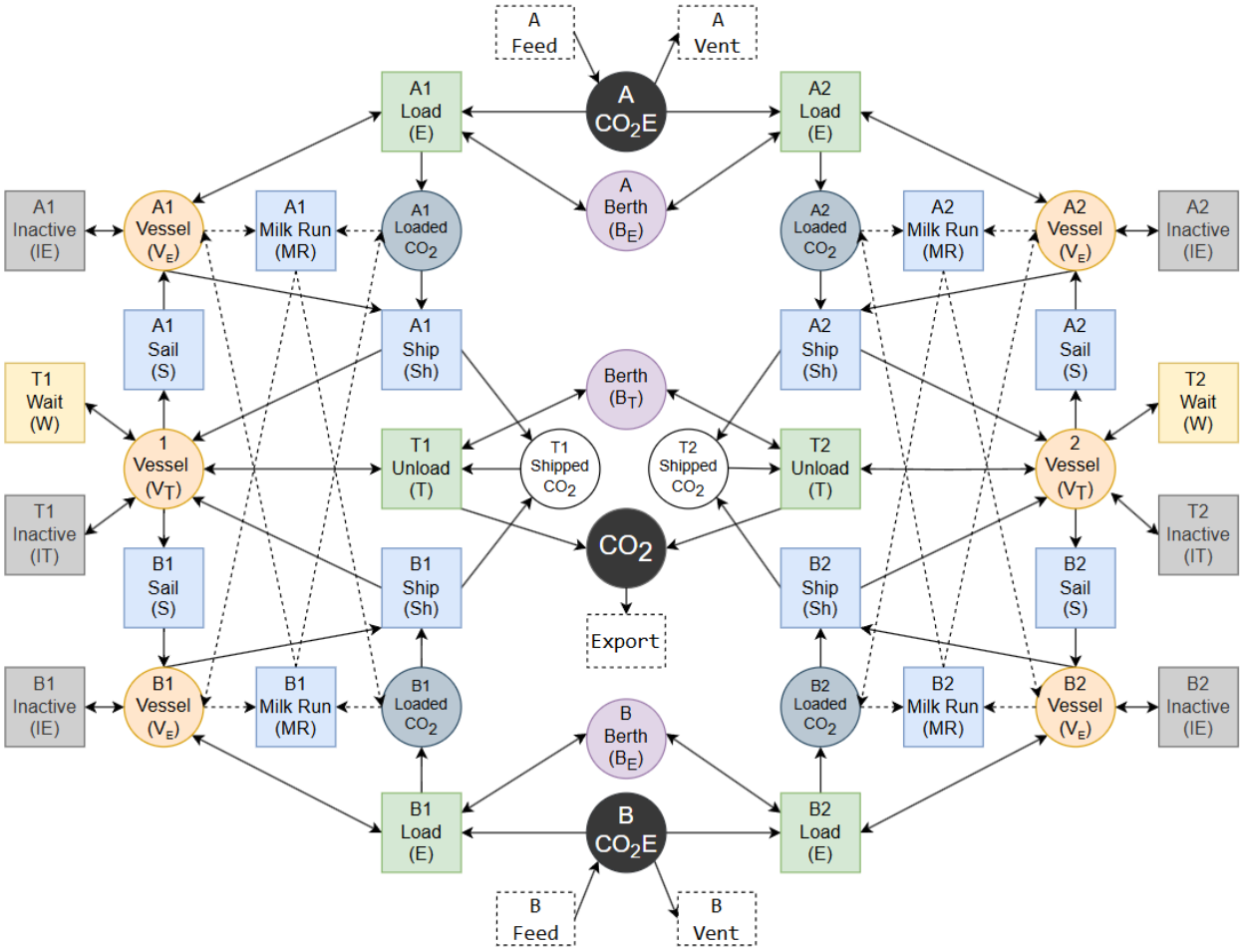

Figure 8: RTN schematic for 2 Vessels and 2 Emitters Model with Milk Runs

6. Numerical Results and Discussion

The computer used for solving the examples is a 2.7GHz AMD Ryzen 7 PRO 6850U CPU laptop with 32 GB of RAM. GAMS/CPLEX 22.1 has been used as the solver for the MILP, which was

modeled with GAMS. We demonstrate the performance of the model on five small examples, and on a real-life instance.

Example 1:

We first consider an example with 1 vessel and 1 emitter for a time horizon of 120 hours. There are no possibilities of milk runs considering only 1 emitter- the simple case. The RTN for this example is depicted in Figure 5. We consider the model parameters of Vessel 1, Emitter A, and of the Injection Terminal, given in Tables 1-3. The vessel starts at the injection terminal port.

The MILP model involves 3,244 equations, 1,422 binary variables and 2,643 continuous variables. Optimality was reached with a CPU time of 0.891 seconds using GAMS/ CPLEX 22.1 for a time horizon of 120 hours with a timestep of 1 hour, as shown in Figure 4. The results are shown in Figures 9-11. Figure 9 depicts the cryogenic CO_2 level at the emitter port and at the injection terminal. The CO_2 profile at the emitter keeps on increasing over the entire horizon, except when the vessel reaches and loads the CO_2 from the emitter port. The injection terminal has an injection rate which is depicted by the decrease in terminal CO_2 level. When the level at the injection terminal reaches 25% of its capacity, the injection rate decreases by 75%. When the vessel starts unloading CO_2 at the injection terminal, the level storage level increases. The vessel does 1 complete voyage to the emitter during the horizon, as it appears in Figure 9.

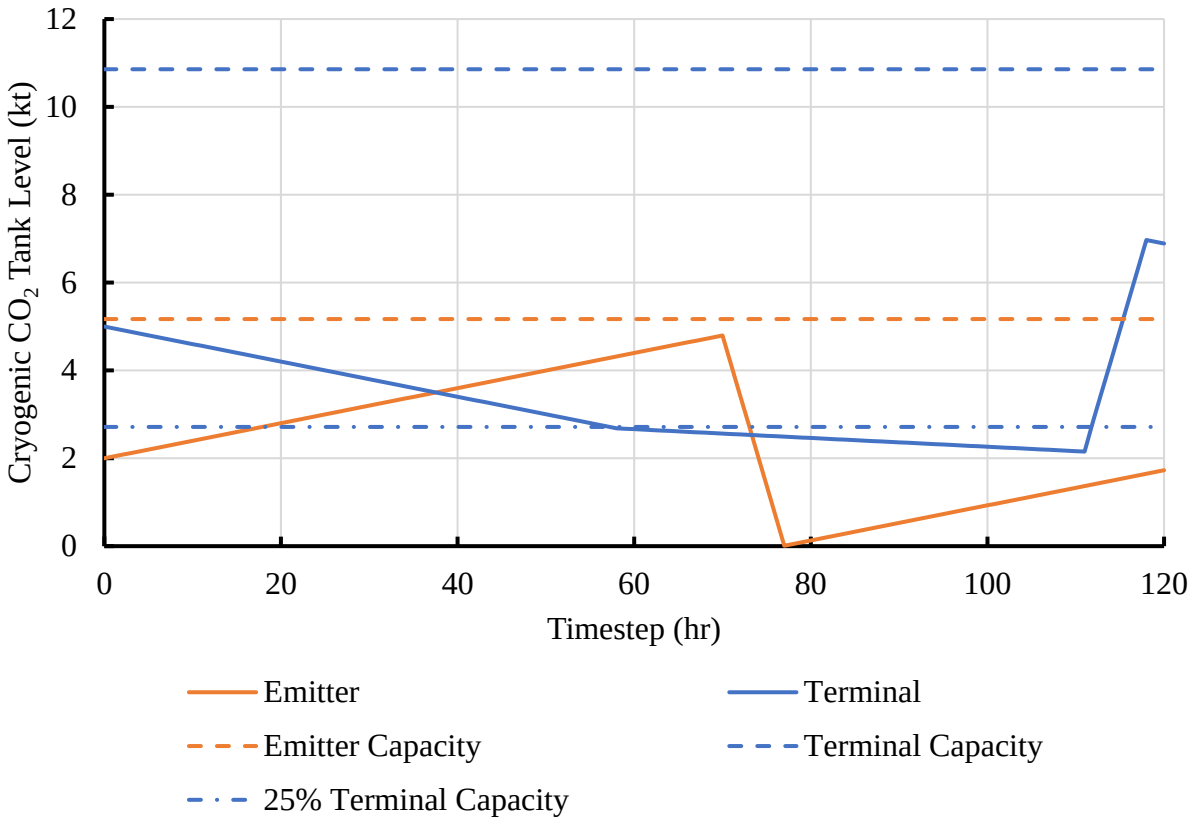

Figure 9: Storage tank profiles at emitters and injection terminal in Example 1

Figure 10 depicts the berths availability at the terminal port, the load profile in the vessel and the amount unloaded from the vessel at the terminal port. When the load increases, the vessel is loading at the emitter port, while when the load decreases, the vessel is unloading at the terminal port as

shown in Figure 10. The vessel is sailing from the emitter to the terminal port when the load profile is constant and non-zero.

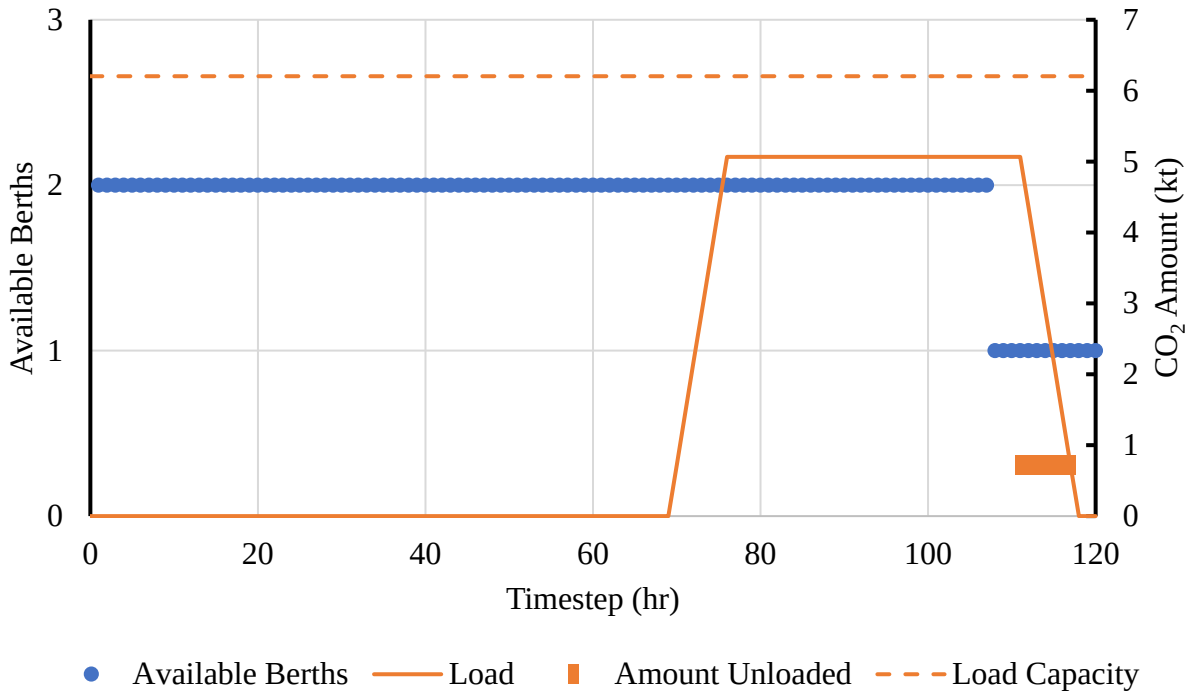

Figure 10: Berths availability and unloading at the injection terminal in Example 1

Figure 11 depicts the Gantt chart for all the tasks done by Vessel 1. Note from Figure 11 that the number of timesteps required for sailing to and from emitter is constant, since we have taken the vessel speed to be constant. Note also that the number of timesteps for loading and unloading are equal, since what is loaded has to be unloaded. The vessel waits at the injection terminal port in the beginning of the horizon and only starts sailing when it can ship the maximum load of CO_2 from the emitter by the end of the horizon.

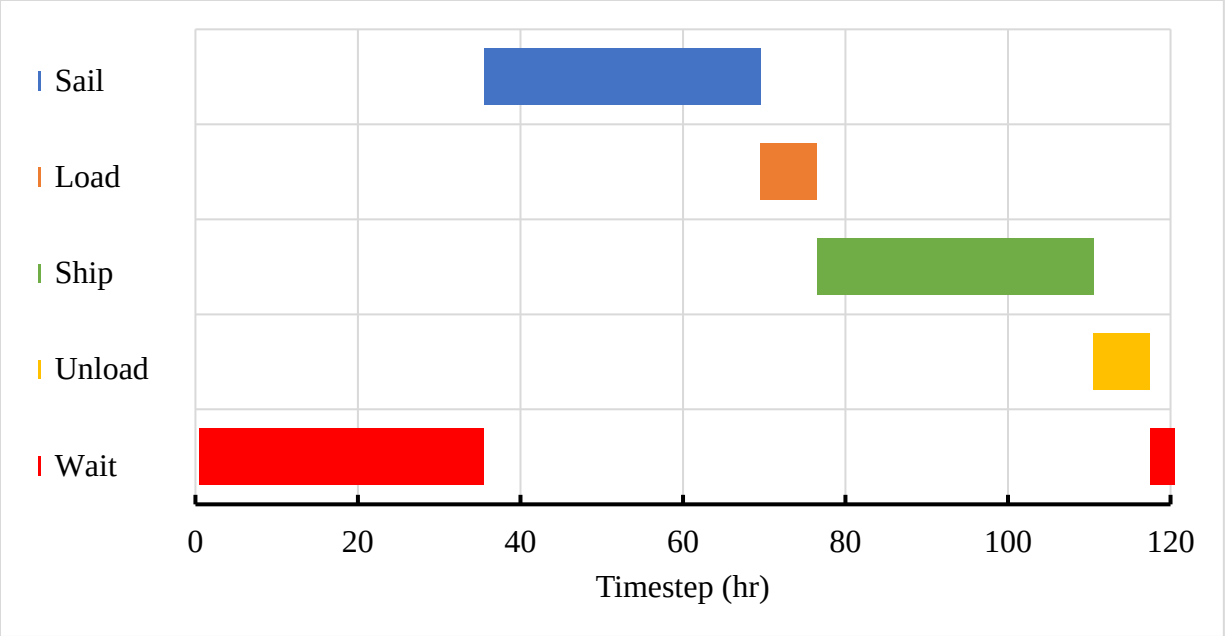

Figure 11: Gantt chart of Example 1

Table 1: Vessels Parameters

	Vessel 1	***Vessel 2***
Vessel Service Speed (Knots)	**10**	
Loading Speed (m^3/hr)	**700**	**1100**
Maximum Loading Capacity (m^3)	**6000**	**9000**
Bunker Tank Capacity (m^3)	**400**	**600**
Fuel Consumption (tons/day)		
Sailing (S)	**10**	**12**
Loading (E)	**2**	**3**
Unloading (T)	**2.5**	**3.5**
Waiting (W)	**1**	**2**
Channeling (Ch)	**3**	**4**
Mooring (M)	**1**	**1.5**
Bunkering (B)	**1**	**1.5**
Contingency (Co)	**2**	**2.5**
$R^{init}_{V_T,j,t}\big\vert_{t=1}$	**1**	**1**
$R^{init}_{V_E,i,j,t}\big\vert_{t=1} \forall i \in I$	**0**	**0**

Table 2: Emitters Parameters

	Emitter A Terminal	*Emitter B Terminal*
Distance from Injection Terminal (km)	**500**	**600**
Distance between Emitters (km)	**85**	
Channeling time (hrs)	**2**	**3**
CO_2 Production (MTPA)	**0.35**	**0.5**
Operational Volume (m^3)	**5,000**	**5,400**
Number of Berths	**1**	**1**

Table 3: Injection Terminal Parameters

	Injection Terminal
Channeling time (hrs)	**2**
Operational Volume (m^3)	**10,500**
Number of Berths	**2**

Example 2:

In this example with one vessel and one emmiter, we solve the previous example with a horizon twice as long of 240 hours. The MILP model involves 6,484 equations, 2,882 binary variables, and 5,283 continuous variables, as shown in Table 4. The model was solved in 20.3 seconds using GAMS/CPLEX 22.1 to optimality. Figure 12 depicts the storage profiles at the emitter and at the injection terminal. When the level at the injection terminal becomes lower than 25% of the capacity, the injection flow rate decreases to 25% its set value. The convex hull reformulation of Equation (34) predicts the injection flow rate as depicted in Figure 12. The vessel does 2 complete voyages to the emitter during the horizon, as it appears in Figure 12, and also in the Gantt chart in Figure 14. Note that from Figure 12 the vessel does not load all the available cryogenic CO_2 at the emitter during loading, since in this model, loading happens in batches, as shown in Equation (17). If the remaining amount is less than the discretized loading amount per timestep, the vessel is unable to load anymore.

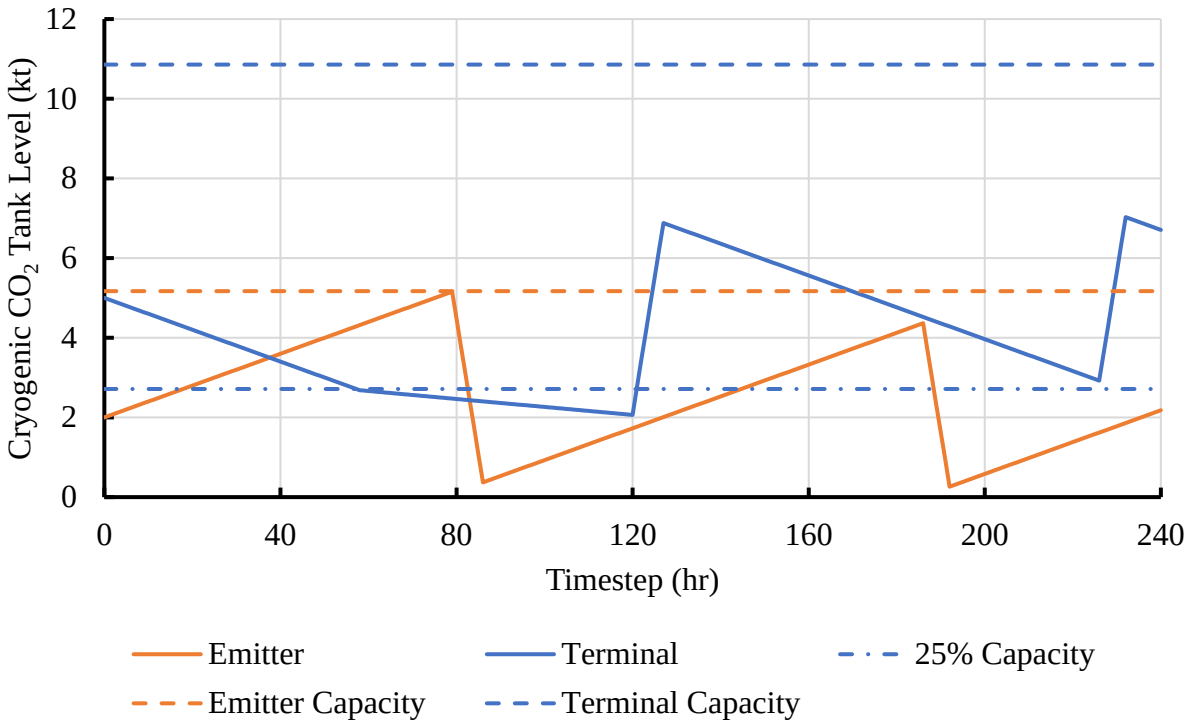

Figure 12: Storage Tank Profiles at Emitters and Injection Terminal in Example 2

Figure 13 depicts berths availability at the injection terminal and the extent of the task *Unload*, $\xi_X|_{j,t}$ along the horizon. Since only one vessel is active, only one berth is consumed at most at every timestep, as shown in Figure 13. Also, the vessel ships varying amounts of cryogenic CO_2 in every voyage.

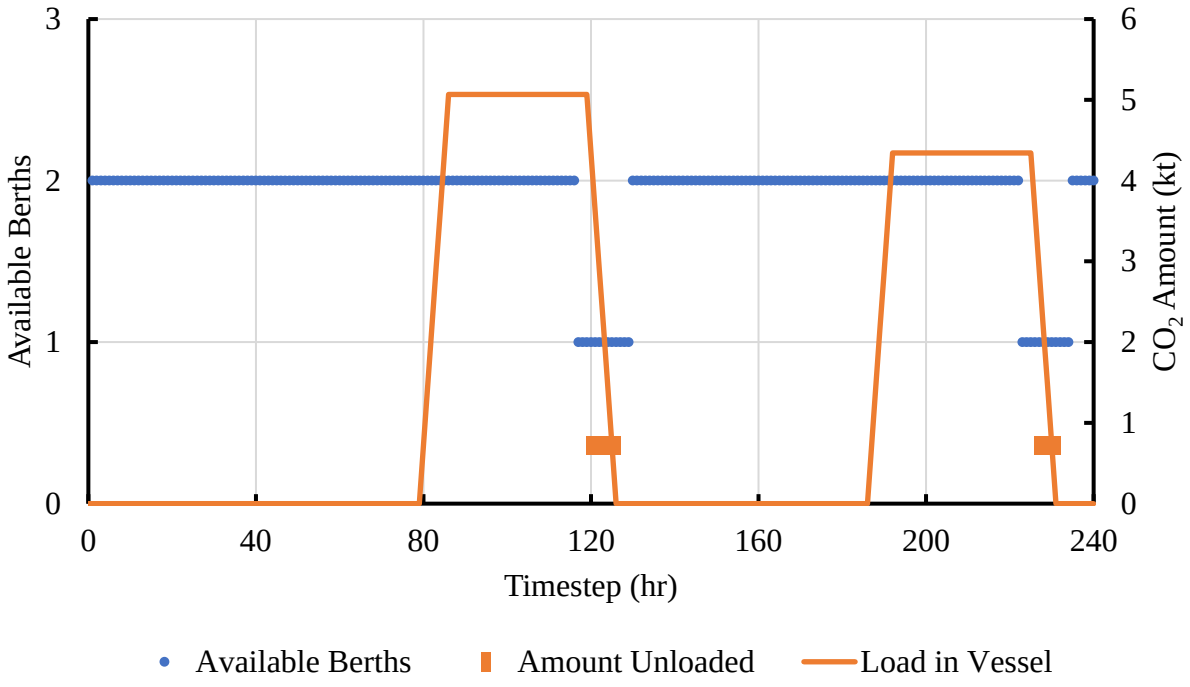

Figure 13: Berths availability and unloading at the injection terminal in Example 2

It is depicted in Figure 14 that the vessel waits at the injection terminal between voyages so that the emitter produces enough cryogenic CO_2 to maximize the shipment by the end of the horizon.

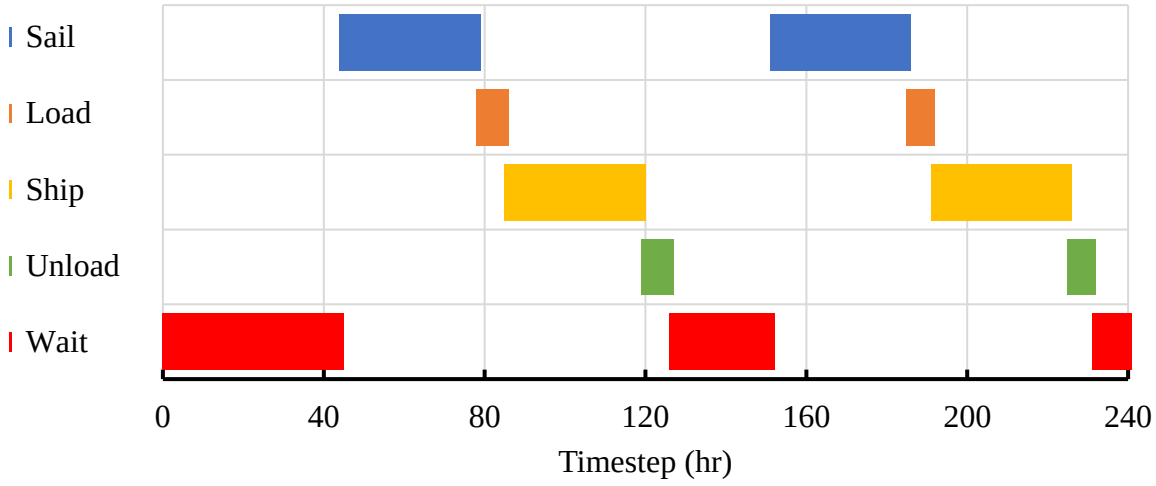

Figure 14: Gantt chart of Example 2

Example 3:

We consider next a third example with 2 vessels and 2 emitters just as depicted in Figure 6, without milk runs. The model parameters for each vessel, emitter and injection terminal are given in Tables 1-3. The two vessels have different capacities. The initial location for the vessels is at the injection terminal. Emitter A is set to only allow the smaller vessel to unload at its berth, while Emitter B allows both vessels 1&2. Both vessels start at the injection terminal port with empty loads. Fuel consumption data in Table 2 are used for Equation (40). The time horizon is set to 120 hours, which is same as in Example 1.The MILP model involves 6,367 equations, 4,446 binary variables, and 5,283 continuous variables as shown in Table 4. The model was solved to optimality in 0.53 seconds using GAMS/ CPLEX 22.1. Figure 15 depicts the storage profiles of each emitter and of the injection terminal, along with the maximum storage capacity at each terminal. As shown in Figure 15, when the level at the injection terminal is below 25% capacity, the injection flow decreases, and the tank does not drain as fast. The tank level at Emitter B reaches its maximum at timestep 45, before loading the cryogenic CO_2 to the vessel. No cryogenic CO_2 is lost from venting since the level does not exceed the maximum capacity.

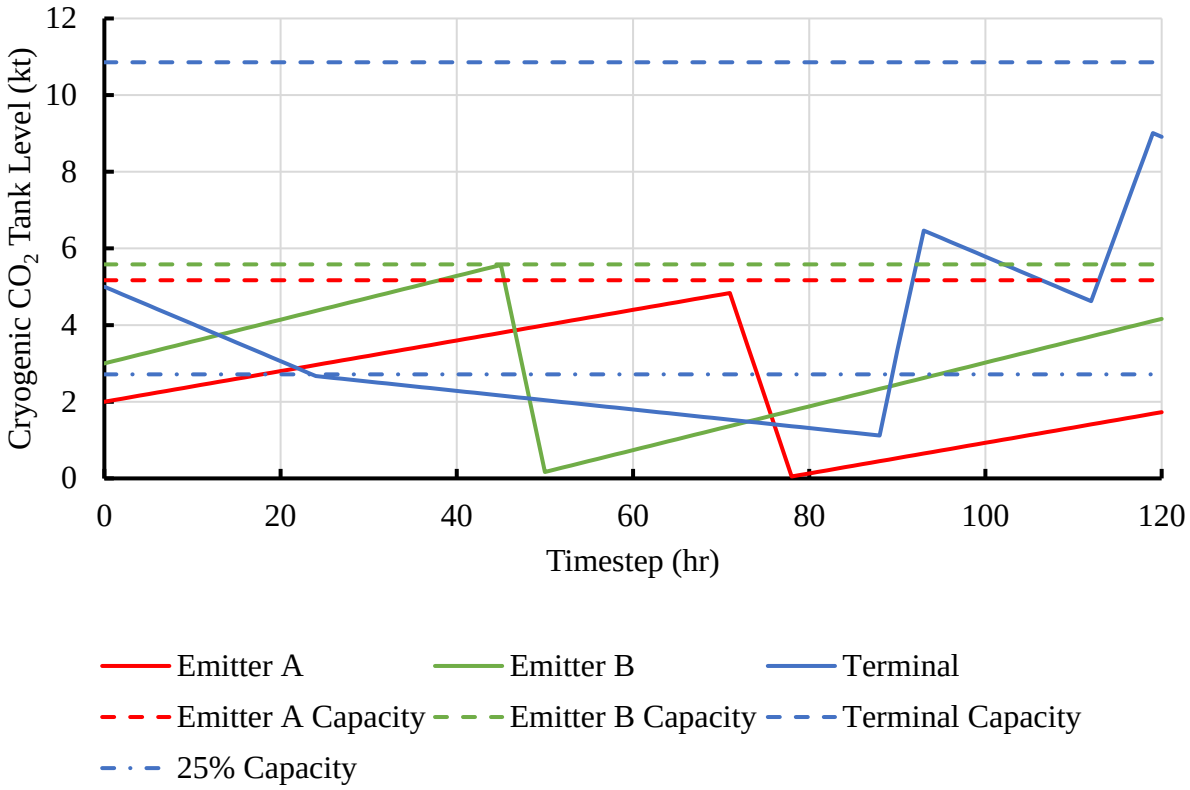

Figure 15: Storage tank profiles at emitters and injection terminal in Example 3

Figure 16 shows the timesteps at which the vessels unload at the injection terminal port. It shows that the vessels do one voyage each. The berth is consumed 3 timesteps before and after unloading, to account for mooring, connection, unmooring, and disconnection, as shown in Figure 16. It can be seen that Vessel 1 takes more timesteps during unloading, but unloads a lower amount of CO_2 than Vessel 2, due to the difference in vessel loading speed.

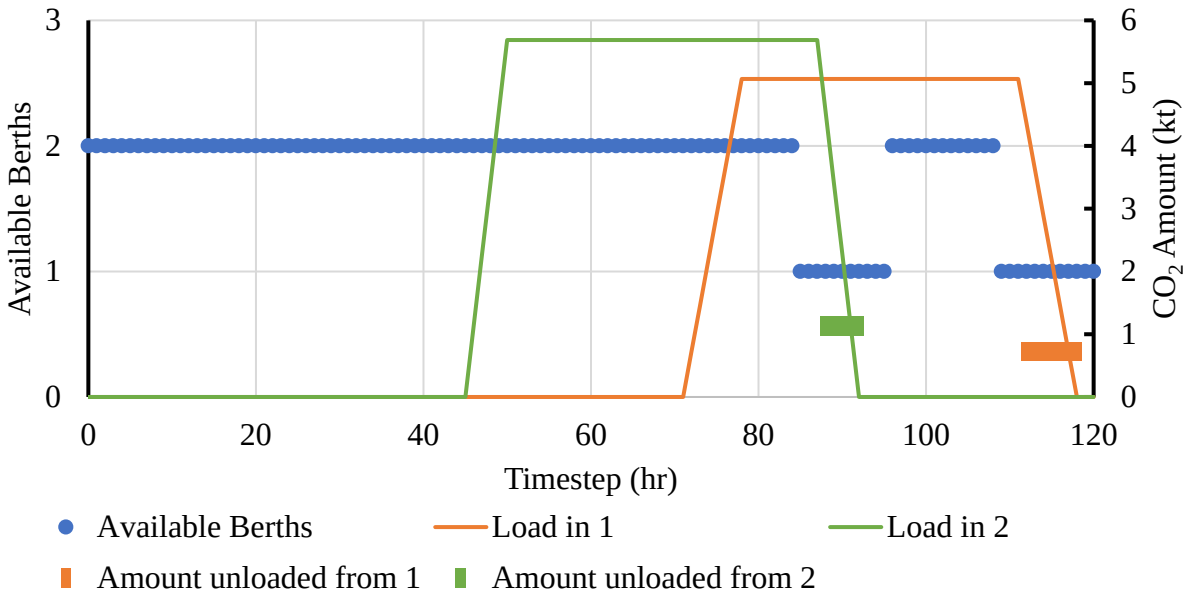

Figure 16: Berths availability and unloading at the injection terminal in Example 3

The Gantt chart of Example 3 in Figure 17 shows Vessel 2 bunkering at the end of the horizon.

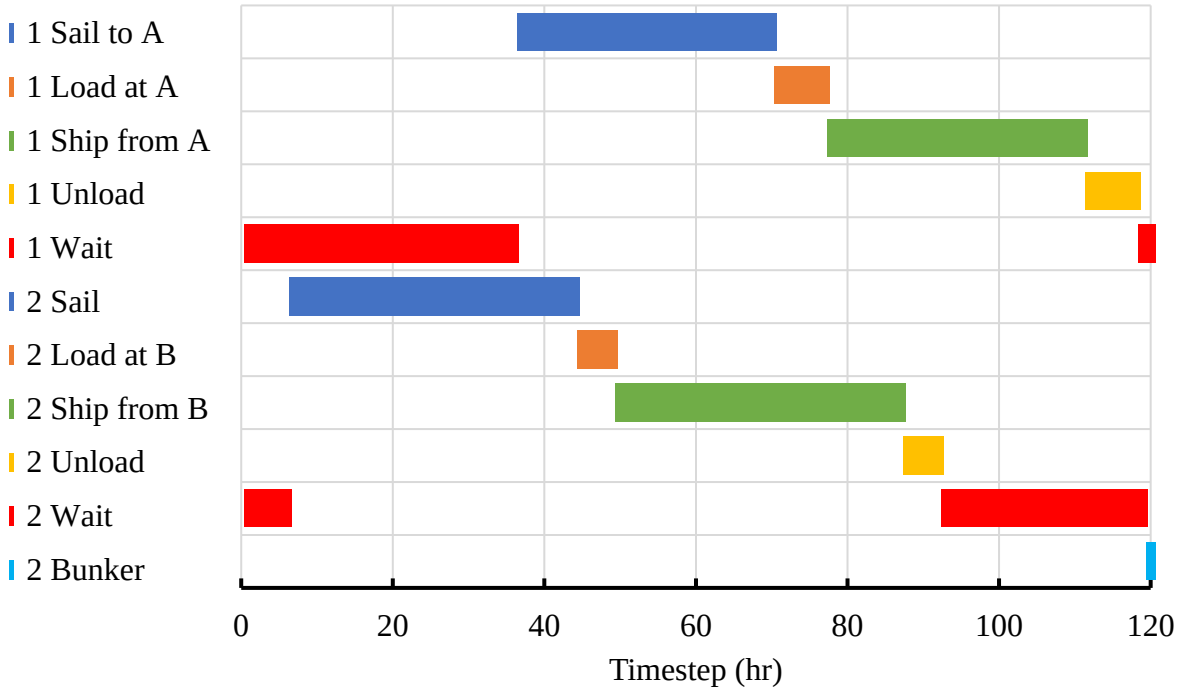

Figure 17: Gantt chart of Example 3

Table 4 summarizes the results of Examples 1, 2, 3, 4, and 5. Example 4 is the same as Example 3 but for a time horizon of 240 hours instead of 120 hours. In the 1 Vessel & 1 Emitter model,

increasing the time horizon from 120 hours to 240 hours increased the CPU time by about 19 seconds. In the 2 Vessels & 2 Emitters model, the CPU time increased by about 265 seconds. Increasing the number of vessels and emitters has a higher impact to the computational time than increasing the time horizon.

Table 4: Problem size and solution of Examples 1, 2, 3, 4, and 5

	Example 1	**Example 2**	**Example 3**	**Example 4**	**Example 5**
	1 vessel & 1 Emitter		2 Vessels & 2 Emitters		
Time Horizon (timesteps)	120	240	120	240	120
Milk Runs	No	No	No	No	Yes
Equations	3,244	6,484	6,367	12,727	7,263
Continuous Variables	2,643	5,283	5,283	10,563	5,763
Binary Variables	1,422	2,882	4,446	8,886	5,406
Objective Function ($\times 10^3$ €)	178.1	327.3	372.1	715.4	398.4
Shipped CO_2 (m^3)	4,900	9,100	10,400	20,100	11,100
CPU Time (sec)	0.89	20.3	0.53	265.4	4.42
LP Relaxation Objective Function ($\times 10^3$ €)	200.4	379.3	484.9	920.8	484.9

Example 5:

We consider next an example with 2 vessels and 2 emitters that considers milk runs, as depicted in Figures 7 and 8. The same model parameters given in Tables 1-3, are used. The MILP model involves 7,263 equations, 5,406 binary variables, and 5,763 continuous variables as shown in Table 5. The model was solved in 4.4 seconds using GAMS/CPLEX 22.1 to optimality for a time horizon of 120 hours with a timestep of 1 hour.

The results are shown in Figures 18-21. Figure 18 depicts the cryogenic CO_2 storage profiles at each emitter terminal and at the injection terminal, along with the maximum storage capacity at each terminal. As shown in Figure 18, the cryogenic CO_2 level at Emitter B drops twice, which means that the emitter is visited by a vessel twice. Since the distance between Emitter A and Emitter B is relatively short, Vessel 1 sails to Emitter B and then does a milk run to Emitter A, as shown in Figure 19 and in the Gantt chart in Figure 20.

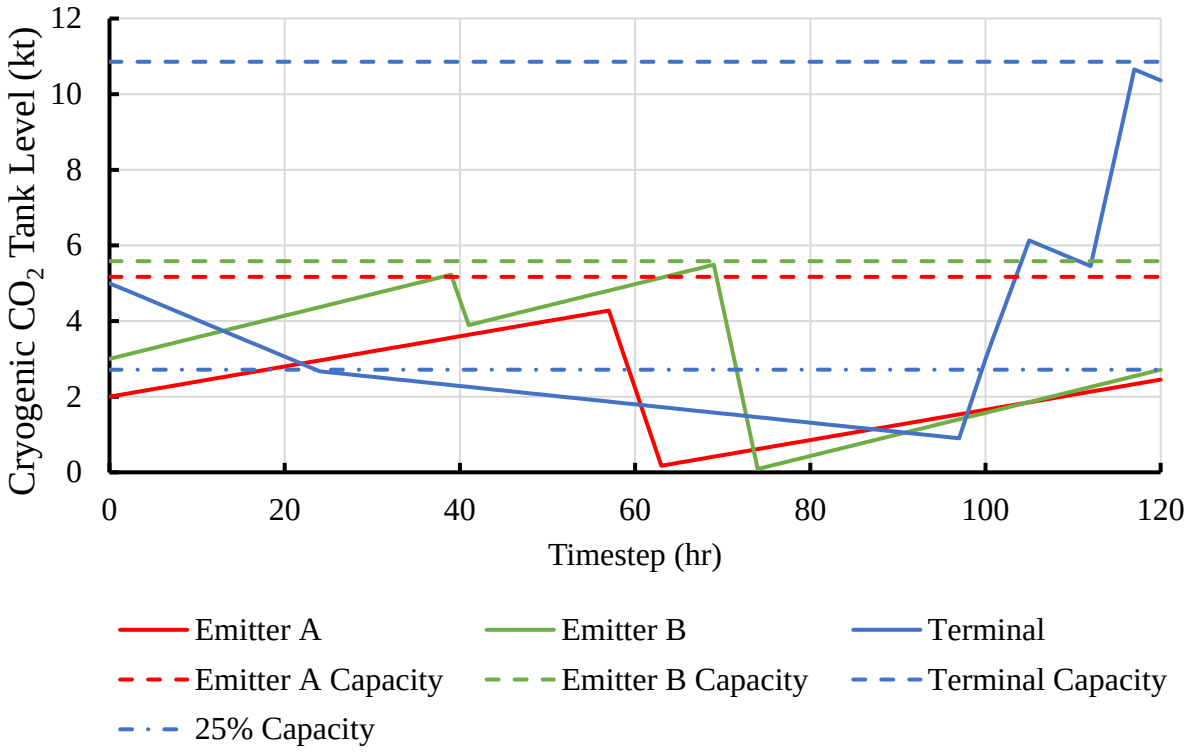

Figure 18: Storage tank profiles at emitters and injection terminal in Example 5

Figure 19 shows the time steps at which the vessels unload at the injection terminal port. It shows that the vessels only do one voyage each, but Vessel 1 loads CO_2 nonconsecutively. This could not happen if it were loading CO_2 from the same port. The Gantt chart in Figure 20 shows how Vessel 1 loads at Emitter B and then loads at Emitter A before sailing to the injection terminal. As shown in Figure 20, Vessel 2 only sails to Emitter B, since Emitter A does not allow the larger vessel. Vessel 2 bunkers at the end of the time horizon, as shown in Figure 20. The amount of fuel bunkered per timestep is discretized to $50\,m^3$. The model that allows milk runs ships more cryogenic CO_2 to the injection terminal with the same amount of timesteps compared to the model

that does not allow milk runs. The optimal value of shipped CO_2 is 11,100 m^3, which is larger than the resulting shipped CO_2 in Example 3, which is 10,400 m^3.

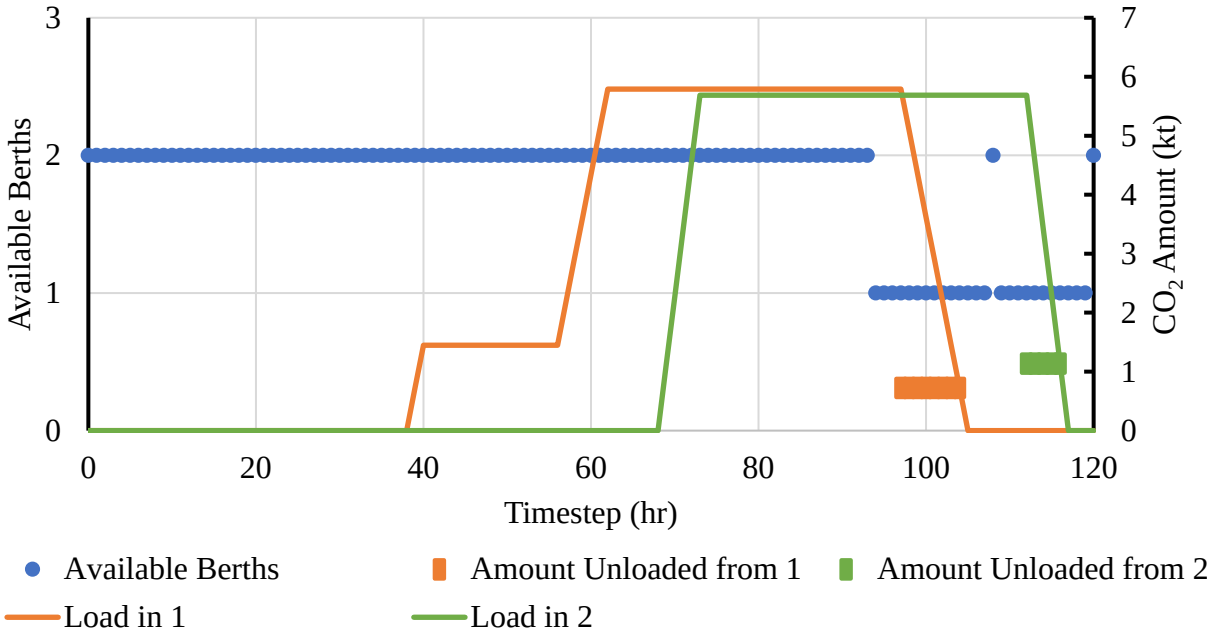

Figure 19: Berths availability and unloading at the injection terminal in Example 5

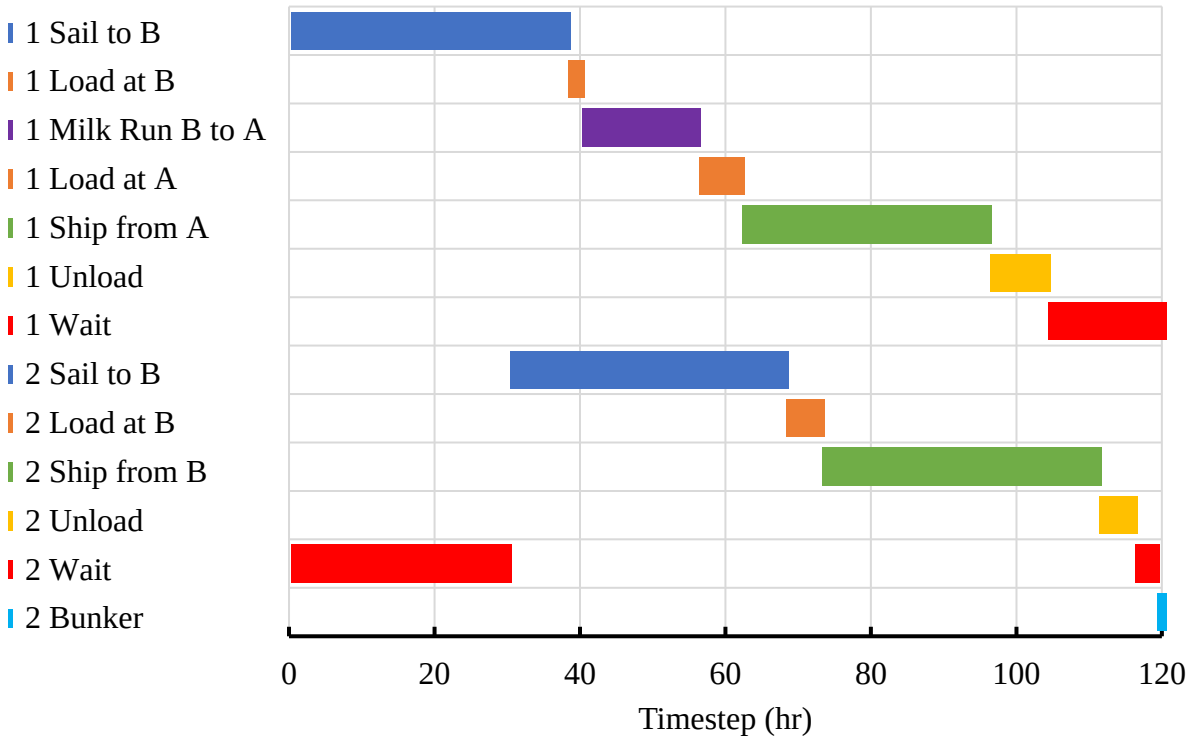

Figure 20: Gantt chart of Example 5

Example 6:

Example 6 represents a real instance from industry of a CO_2 transportation system from which the model parameters were obtained. It involves 3 emitters, one injection terminal, and 4 equivalent vessels. The model was solved using GAMS/CPLEX 22.1 for a time horizon of 120 hours with a timestep of 1 hour. The model size is large with 18,055 equations, 16,456 binary variables and 14,043 continuous variables, and was solved to the optimality gap of 0.1% after 1,794 seconds as shown in Table 5.

Table 5: Problem size and solution of Example 6

Example 6	**4 Vessels & 3 Emitters**
Time Horizon (timesteps)	120
Equations	18,055
Continuous Variables	14,043
Binary Variables	16,456
Objective Function ($\times 10^3$ €)	503.7
Optimality Gap (%)	0.1
Shipped CO_2 (m^3)	21,600
CPU Time (sec)	1,794
LP Relaxation Objective Function	654.1

Figure 21 shows the storage profiles at the emitters with the respective tank capacity and at the injection terminal. No CO_2 amount is lost from venting, since none of the storage tanks had to exceed capacity, as shown in Figure 21. It is evident Emitter C is visited by a vessel twice since the loading happens inconsecutively. From the Gantt chart in Figure 23, it is depicted that Emitter C is visited by Vessels 1 and 4. It can be deduced from Figure 21 that the vessels unload during

the end of the time horizon, as shown with the increase in injection terminal tank level, and with the unloading task occurrences in Figure 22.

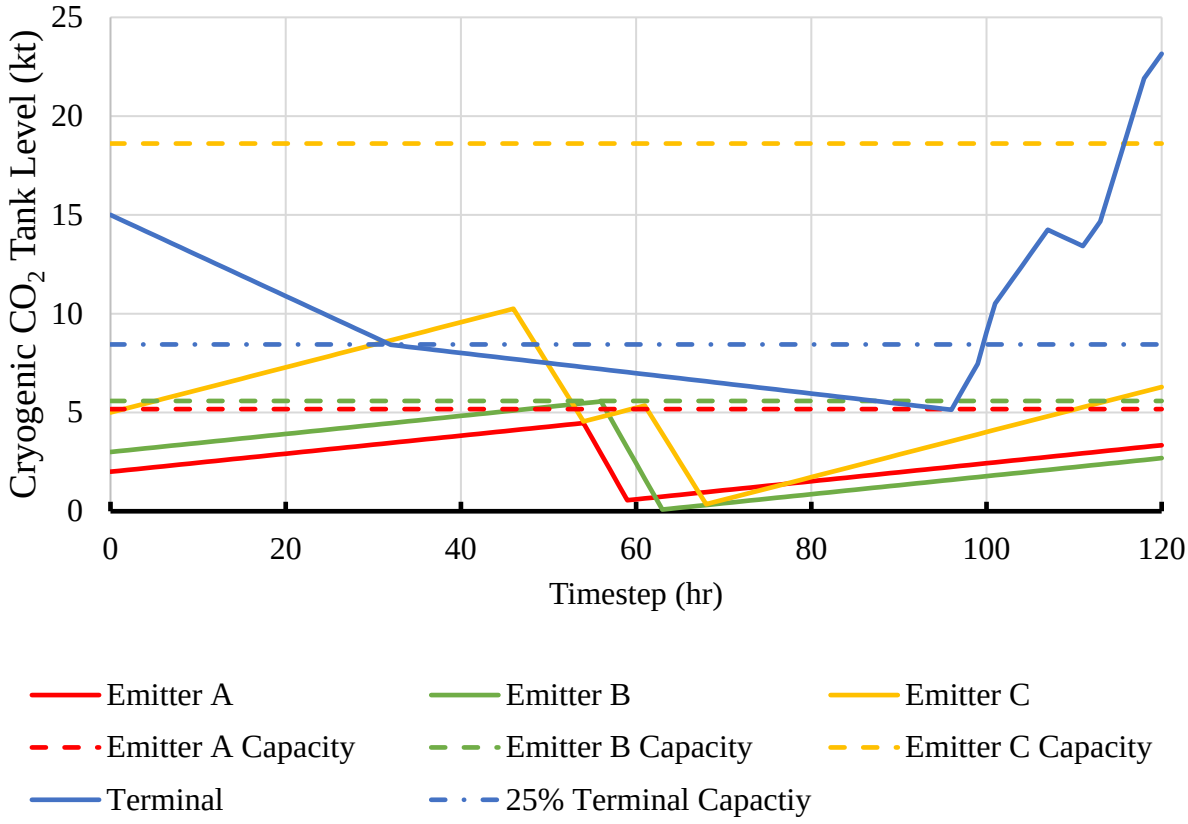

Figure 21: Storage tank profiles at emitters and injection terminal in Example 6

Figure 22 shows that the vessels consume the two available berths during the end of the horizon, when the vessels arrive to the injection terminal port. The shipment of CO_2 is scheduled so as to not consume more than the two available berths at any timestep. It is depicted in Figure 22 that each vessel loads various amounts of cryogenic CO_2 and that none of the loads reach the maximum loading capacity.

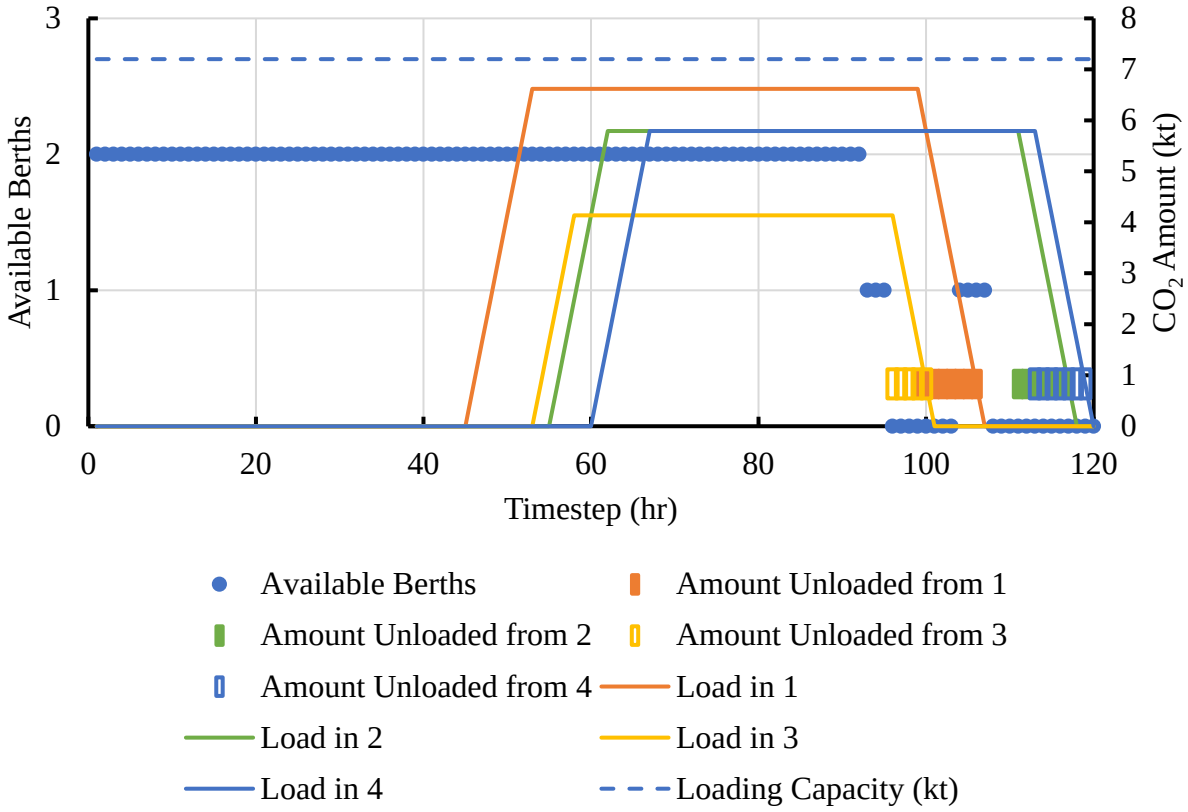

Figure 22: Berths availability and unloading at the injection terminal in Example 6

Figure 23 shows the Gantt chart for all the vessels and tasks assigned to each vessel at each timestep. It is depicted that the vessels spend most of the timesteps sailing to and from the emitters, due to the long distance between emitters and the injection terminal.

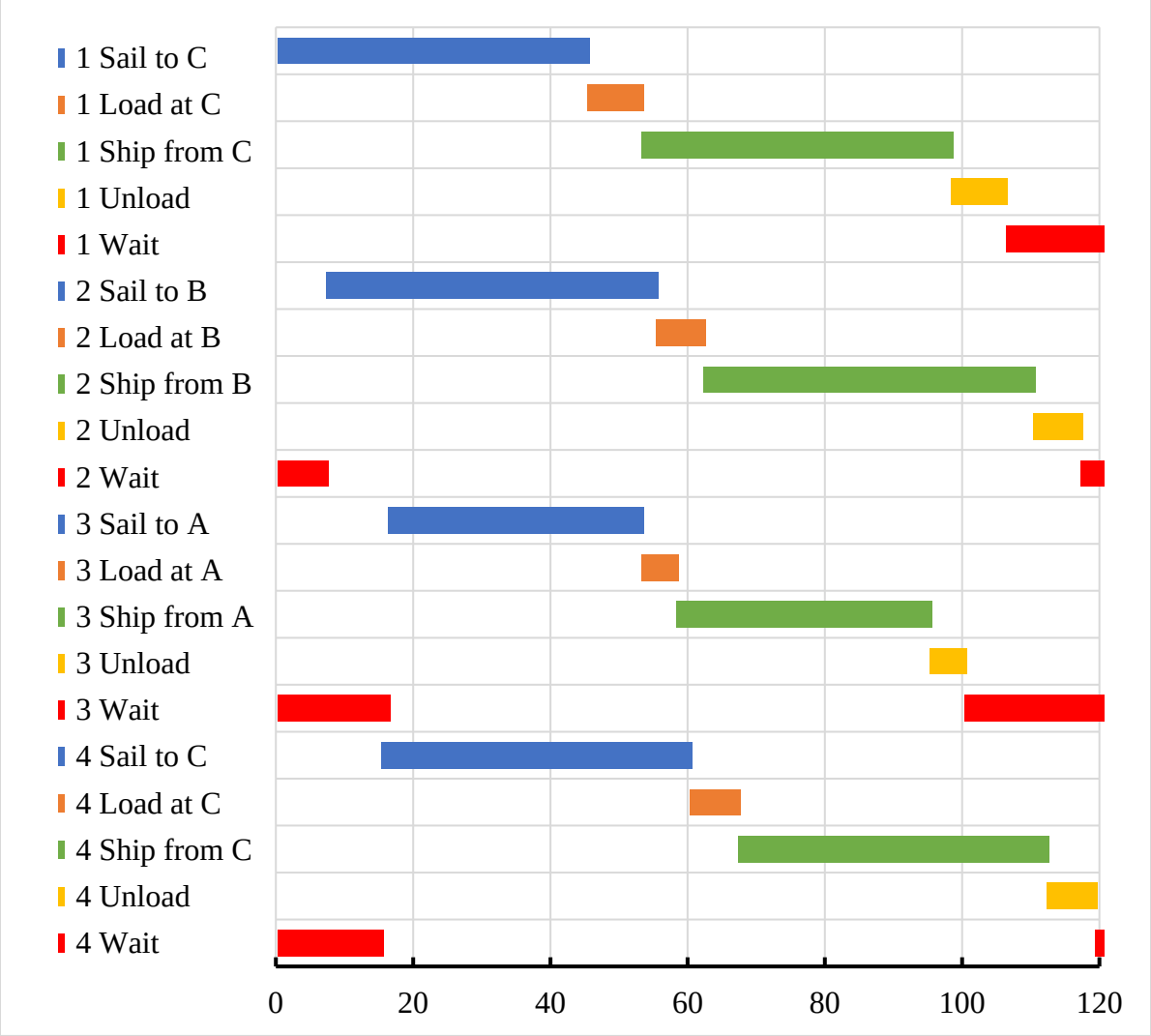

Figure 23: Gantt chart of Example 6

Figure 24 depicts Equation (40) in Example 3, showing the bunker tank level profiles for each vessel. As depicted in Figure 24, the bunker tank level for Vessel 3 at the end of the horizon is

higher than the rest and that is because of the shorter distance it takes to get to Emitter A from the injection terminal.

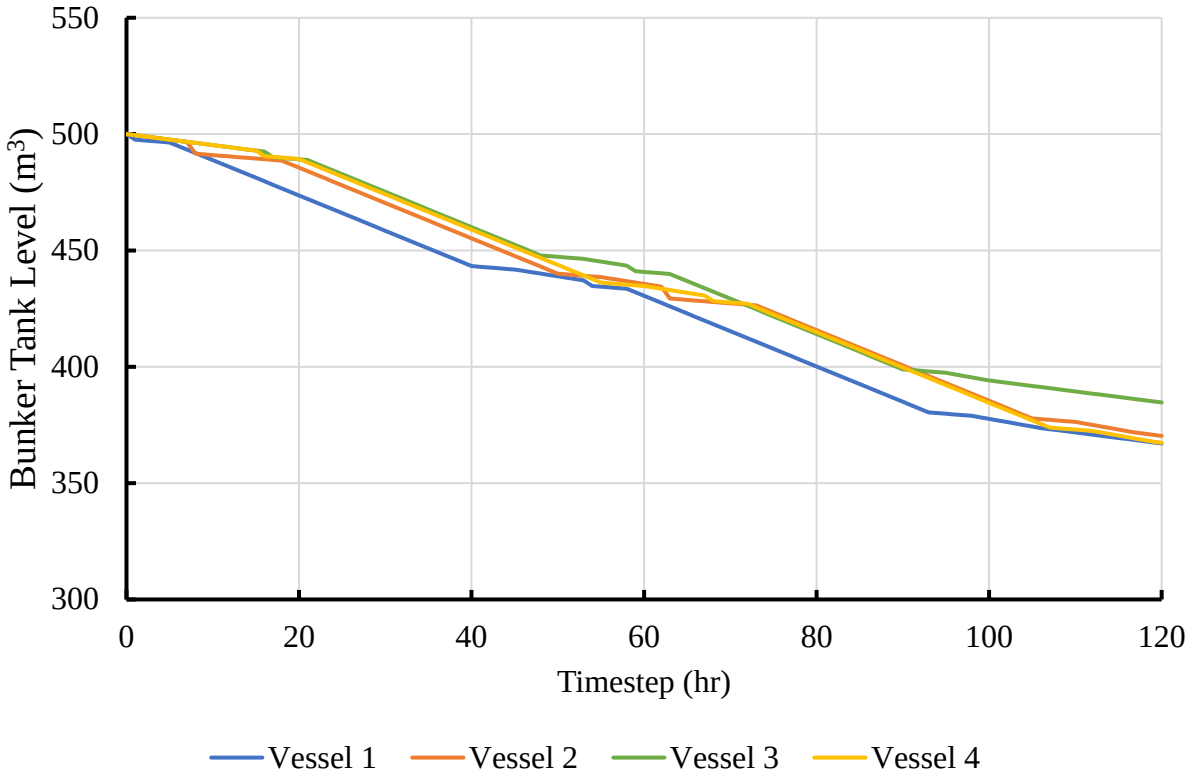

Figure 24: Bunker tank level profile in Example 6

7. Conclusions and future work

We have presented an MILP model for the optimal shipment scheduling of CO_2 carriers for CCUS systems, maximizing the revenue of CCUS systems and minimizing the fuel expenses of transportation and venting at the emitters and injection site. The extended RTN scheduling model has been applied to the shipment scheduling process on five small-scale examples, and on one large-scale real life instance. The results of the model for real-life data show detailed scheduling of the vessels during each hour over a horizon of over a week and inventory management at the emitter ports. This model accounts for all the major operations, such as mooring, channeling, and ramping in/out.

There is a limitation, however, that arises when scaling the model to larger instances over longer time horizons that is its intractability. To address this, decomposition methods have been explored and are discussed in detail in a follow-up paper by Shikha et al.[19] These methods allow the optimization of larger instances that include more vessels and more emitters making it more suitable for CCUS hubs. A longer horizon would allow for seasonality of each emitter's CO_2 production rate.

Finally, for future work, the model could be expanded to include emitter port closures during the night and allowing only time windows during which the vessel can load or unload. The RTN model can also consider variable sailing speed to reduce fuel consumption and increase flexibility in scheduling unloading with limited berth availability. In addition, estimating carbon dioxide emissions would be a valuable expansion to the model.

Acknowledgments

We are most grateful to TotalEnergies for their financial support and for providing a description of the industrial use case along with the optimization problem at stake. Additionally, we appreciate the financial support from the Center for Advanced Process Decision-Making (CAPD) at Carnegie Mellon University. Finally, we appreciate the help of Dr. Hector D. Perez in the development of the extended RTN model.

Nomenclature

$i \in I$	emitters
$i \in I^{lv}$	emitters with berth(s) that only accept(s) large vessels
$i \in I^{sv}$	emitters with berth(s) that only accept(s) small vessels
$j \in J$	vessels
$j \in J^{lv}$	large vessels with high capacity
$j \in J^{sv}$	small vessels with low capacity
$t \in TP$	timesteps
$o \in O$	operations

Parameters:

TI	Duration of timestep (hr)
τ_{PBP}	Timesteps required for operations before and after loading/unloading upon reaching the Pilot Boarding Point (PBP) that include awaiting pilot, mooring in/out, ramping in/out, and contingency $= \left\lceil \frac{2(0.5+2+1)+1}{TI} \right\rceil = \left\lceil \frac{8}{TI} \right\rceil$
τ_{BO}	Timesteps required for operations before and after loading/unloading during which the berth is occupied, that include mooring in/out and ramping in/out $= \left\lceil \frac{2(2+1)}{TI} \right\rceil = \left\lceil \frac{6}{TI} \right\rceil$
ST_i	Timesteps required for sailing between Pilot Boarding Points of emitter i (PBP_i) and of the terminal port (PBP_T)
CT_i	Timesteps required for channeling at emitter i
CT_T	Timesteps required for channeling at injection terminal port
$\tau_{s,i}$	Timesteps required for the vessel to get from the berth of emitter i to the berth at terminal port or vice versa $= \tau_{PBP} + ST_i + CT_i + CT_T$
$ST_{i,i'}$	Timesteps required for sailing between Pilot Boarding Points of emitter i (PBP_i) and of emitter i' ($PBP_{i'}$)
$\tau_{i,i'}$	Timesteps required for the vessel to get from the berth of emitter i to the berth emitter i' $= \tau_{PBP} + ST_{i,i'} + CT_i + CT_{i'}$
τ_M	Timesteps required for mooring at arrival to loading/unloading port $= \left\lceil \frac{2}{TI} \right\rceil$
LS_j	Loading speed of vessel j
C_j	Storage capacity of vessel j
C_i	Storage capacity at emitter i
C_T	Storage capacity at the injection terminal
$B_{E,i}^{max}$	Maximum number of berths available at emitter i
$B_{T,i}^{max}$	Maximum number of berths available at injection terminal port

$\Pi^{in}_{CO_2,E_{i,t}}$	Produced cryogenic CO_2 at emitter i in time step t
FP	Fuel price of LNG
$C_{o,j}$	Fuel consumption in LNG equivalent for vessel j (ton per hour) during operation o

Binary Variables:

x_t	Binary indicating if terminal storage tank level is below 25% capacity
$y_{i,j}$	Binary indicating if vessel j is assigned to emitter i
z_j	Binary indicating if vessel j is active
$N_{E,i,j,t}$	Binary indicating if vessel j is loading at emitter i during timestep t
$N_{Sh,i,j,t}$	Binary indicating if vessel j started shipping from emitter i at timestep t
$N_{S,i,j,t}$	Binary indicating if vessel j started sailing to emitter i at timestep t
$N_{IE,i,j,t}$	Binary indicating if vessel j is inactive at emitter i during timestep t
$N_{Sh,i,j,t}$	Binary indicating if vessel j started shipping from emitter i at timestep t
$N_{T,j,t}$	Binary indicating if vessel j is unloading at Terminal during timestep t
$N_{W,j,t}$	Binary indicating if vessel j is waiting at Terminal during timestep t
$N_{IT,j,t}$	Binary indicating if vessel j is inactive at Terminal during timestep t
$N_{B,j,t}$	Binary indicating if vessel j is bunkering at Terminal during timestep t
$N_{MR,i,i',j,t}$	Binary indicating if vessel j leaves emitter i to emitter i' for a milk run at timestep t

Positive Variables:

$\Pi^{out}_{CO_2E,i,t}$	vented CO_2 at emitter i during time step t
$R_{CO_2E,i,t}$	CO_2 level in the tanks at emitter i at time step t
$R_{B_E,i,t}$	berth availability at emitter i at time step t
$R_{V_E,i,j,t}$	vessel j at emitter i at time step t
$R_{L,i,j,t}$	loaded CO_2 from emitter i to vessel j at time step t
$R_{V_T,j,t}$	shipped vessel j at Terminal port at time step t
$R_{Shipped,j,t}$	shipped CO_2 by vessel j at terminal port at time step t
$R_{B_T,t}$	berth availability at terminal port i at time step t
$R_{LF,t}$	loaded Fuel in vessel j at time step t
$R_{F,t}$	Fuel available at the Terminal port
$R_{CO_2,t}$	CO_2 level in the tanks at terminal port i at time step t

$R_{CAP,j,t}$	available capacity in vessel j at timestep t
$OPEX_{j,t}$	fuel costs for vessel j during timestep t
$\Pi^{out}_{CO_2,i,t}$	CO_2 injection from the injection terminal storage tanks
$\xi_{E,i,j,t}$	amount of CO_2 loaded during timestep t at emitter i
$\xi_{Sh,i,j,t}$	amount of CO_2 that started to ship at the timestep t
$\xi_{MR,i,i',j,t}$	amount of CO_2 that is loaded while vessel j leaves emitter i to emitter i' for a milk run at timestep t
$\xi_{T,j,t}$	amount of CO_2 unloaded during timestep t

References:

(1) Abhijnan A.; Desai K.; Wang J.; Rodríguez-Martínez A.; Dkhili N.; Jellema R. Grossmann I. E. Mixed-Integer Nonlinear Programming Model for Optimal Field Management for Carbon Capture and Storage. *Ind. Eng. Chem. Res.* 2024. 63(27), 12053-12063. DOI: 10.1021/acs.iecr.4c00390

(2) Brønmo, G.; Christiansen, M.; Fagerholt, K.; Nygreen, B. A multi-start local search heuristic for ship scheduling—a computational study. *Computers & Operations Research*. 2007, 34(3), 900–917. DOI: 10.1016/j.cor.2005.05.017

(3) Castro, P.M.; Barbosa-Póvoa, A.P. Matos, H.A. Optimal Periodic Scheduling of Batch Plants Using RTN-Based Discrete and Continuous-Time Formulations: A Case Study Approach. *Ind. Eng. Chem. Res.* 2003. 42(14), 3346–3360. DOI: 10.1021/ie0203781

(4) CCUS in Clean Energy Transitions – analysis, 2020. https://www.iea.org/reports/ccus-in-clean-energy-transitions (accessed May 1, 2024).

(5) Christiansen, M.; Fagerholt, K.; Nygreen, B.; Ronen, D. 2013. Ship routing and scheduling in the new millennium. *Eur. J. Oper. Res.* 228(3), 467–483. DOI: 10.1016/j.ejor.2012.12.002

(6) Decarre, S.; Berthiaud, J.; Butin, N.; Guillaume-Combecave, J.-L. CO2 maritime transportation. *International Journal of Greenhouse Gas Control.* 2010. 4(5), 857–864. DOI: 10.1016/j.ijggc.2010.05.005

(7) Floudas, C.A.; Lin, X. Continuous-time versus discrete-time approaches for scheduling of chemical processes: a review. *Comput. Chem. Eng.* 2004. 28, 2109–2129. DOI: 10.1016/j.compchemeng.2004.05.002

(8) Gatica, R.A.; Miranda, P.A. Special Issue on Latin-American Research: A Time Based Discretization Approach for Ship Routing and Scheduling with Variable Speed. *Netw. Spat. Econ.* 2011. 11, 465–485. DOI: 10.1007/s11067-010-9132-9

(9) Georgiadis, G.P.; Elekidis, A.P.; Georgiadis, M. Optimization-Based Scheduling for the Process Industries: From Theory to Real-Life Industrial Applications. *Processes.* 2019. 7(7), 438. DOI: 10.3390/PR7070438

(10) Grossmann, I.E.; Trespalacios, F. Systematic modeling of discrete-continuous optimization models through generalized disjunctive programming. *AIChE J.* 2013. 59(9), 3276–3295. DOI: 10.1002/aic.14088

(11) Harjunkoski, I.; Maravelias, C.T.; Bongers, P.; Castro, P.M.; Engell, S.; Grossmann, I.E.; Hooker, J.; Méndez, C.; Sand, G.; Wassick, J. Scope for industrial applications of production scheduling models and solution methods. *Comput. Chem. Eng.* 2014. 62, 161–193. DOI: 10.1016/j.compchemeng.2013.12.001.

(12) Kim, H.-J.; Chang, Y.-T.; Kim, K.-T.; Kim, H.-J. An epsilon-optimal algorithm considering greenhouse gas emissions for the management of a ship's bunker fuel. *Transp. Res. Part D: Trans. Environ.* 2012. 17(2), 97–103. DOI: 10.1016/j.trd.2011.10.001

(13) Kondili, E.; Pantelides, C.C.; Sargent, R.W.H. A general algorithm for short-term scheduling of batch operations—I. MILP formulation. *Comput. Chem. Eng.* 1993. 17(2), 211–227. DOI: 10.1016/0098-1354(93)80015-F

(14) Li, C.-L.; Pang, K.-W. An integrated model for ship routing and berth allocation. *International Journal of Shipping and Transport Logistics.* 2011. 3(3), 245–260. DOI: 10.1504/IJSTL.2011.040797

(15) Méndez, C.A.; Cerdá, J.; Grossmann, I.E.; Harjunkoski, I.; Fahl, M. State-of-the-art review of optimization methods for short-term scheduling of batch processes. *Comput. Chem. Eng.* 2006. 30, 913–946. DOI: 10.1016/j.compchemeng.2006.02.008

(16) Nie, Y.; Biegler, L.T.; Wassick, J.M.; Villa, C.M. Extended Discrete-Time Resource Task Network Formulation for the Reactive Scheduling of a Mixed Batch/Continuous Process. *Ind. Eng. Chem. Res.* 2014. 53(43), 17112–17123. DOI: 10.1021/ie500363p

(17) Pantelides, C.C. Unified frameworks for optimal process planning and scheduling. In *Proceedings on the Second Conference on Foundations of Computer Aided Operations*. Cache Publications New York, 1994. pp 253–274.

(18) Perez, H.D.; Amaran, S.; Erisen, E.; Wassick, J.M.; Grossmann, I.E. Optimization of extended business processes in digital supply chains using mathematical programming. *Comput. Chem. Eng.* 2021. 152, 107323. DOI: 10.1016/j.compchemeng.2021.107323

(19) Shikha, S.; Guisso J.; Robert A.; Dkhili N.; Laurell A.; Grossmann, I. E. Supply Logistics of Carbon Dioxide in the Optimal Field Management of Carbon Capture and Storage. manuscript in preparation. 2024.

(20) Song, J.-H.; Furman, K.C. A maritime inventory routing problem: Practical approach.

Comput. Oper. Res. 2013. 40(3), 657–665. DOI: 10.1016/j.cor.2010.10.031

(21) Wassick, J.M.; Ferrio, J. Extending the resource task network for industrial applications. *Comput. Chem. Eng.* 2011. 35(10), 2124–2140. DOI: 10.1016/j.compchemeng.2011.01.010

(22) Yee, K.L.; Shah, N. Improving the efficiency of discrete time scheduling formulation. *Comput. Chem. Eng.* 1998. 22(1), S403–S410. DOI: 10.1016/S0098-1354(98)00081-7

(23) Zeng, Q.; Yang, Z. Model Integrating Fleet Design and Ship Routing Problems for Coal Shipping. In *Computational Science – ICCS 2007*. Springer, Berlin, Heidelberg, 2007; Vol. 4489, pp 1000–1003. DOI: 10.1007/978-3-540-72588-6_160